An Automatic Depth Control System for the

On-the-Go Soil Strength Sensor

Except where reference is made to the work of others, the work described in this thesis is my own or was done in collaboration with my advisory committee. This thesis does not include proprietary or classified information.

Clifford Warren Smith, Jr.

Certificate of Approval:

Randy L. Raper, Co-Chair
Affiliate Professor
Biosystems Engineering

John Y. Hung, Co-Chair
Professor
Electrical & Computer Engineering

Lloyd S. Riggs
Professor
Electrical & Computer Engineering

George T. Flowers
Interim Dean
Graduate School

An Automatic Depth Control System for the On-the-Go Soil Strength Sensor

Clifford Warren Smith, Jr.

A Thesis

Submitted to

the Graduate Faculty of

Auburn University

in Partial Fulfillment of the

Requirements for the

Degree of

Master of Science

Auburn, Alabama
December 17, 2007

An Automatic Depth Control System for the

On-the-Go Soil Strength Sensor

Clifford Warren Smith, Jr.

Permission is granted to Auburn University to make copies of this thesis at its discretion, upon the request of individuals or institutions and at their expense. The author reserves all publication rights.

_____

Signature of Author

_____

Date of Graduation

Vita

Clifford Warren Smith, Jr., son of Clifford W. Smith and Patricia L. Smith, was born January 23, 1971 in Northfork, West Virginia. He graduated in 1989 from Mount View High School in Welch, West Virginia. He entered the United States Army in 1989 and served in Desert Shield/Desert Storm in 1990-1991. He entered Alabama Southern Community College in 1998, where he received an Associate of Science degree in May 2000. He entered Auburn University in 2000, where he received a Bachelor of Engineering degree in Electrical and Computer Engineering in May 2003. He entered the Graduate School at Auburn University in August 2003.

Thesis Abstract

An Automatic Depth Control System for the On-the-Go Soil Strength Sensor

Clifford Warren Smith, Jr.

Master of Science, December 17, 2007
(B.S., Auburn University, 2003)
(A.S., Alabama Southern Community College, 2000)

89 Typed Pages

Directed by John Y. Hung and Randy L. Raper

Hardpans are areas of soil compaction formed by vehicle traffic or natural processes. These compacted areas beneath the topsoil can hinder successful crop production. A novel sensor for measuring soil strength was presented in an earlier work, and patented as the OSSS (On-The-Fly Soil Strength Sensor). The focus of this thesis is the design and evaluation of a control system for this new method of sensing soil strength. The graphical user interface has been implemented with National Instrument's LabVIEW ® software, and drives an analog PID-type (proportional, integral, and derivative) position controller for a hydraulic cylinder. This controller causes the strength sensor to vertically oscillate in the soil at consistently spaced distance intervals, regardless of tractor speed variations. Successful development enables this system to collect soil strength information over an entire field at all desired depths in a short period of time.

Acknowledgments

First and foremost I would like to thank Our LORD and Savior Jesus Christ, from whom all blessings flow. And I would like to express my gratitude to the members of the graduate committee, who supervised the thesis project; Mr. Bob Washington, Supervisory Agricultural Engineer, for assistance with frame design; Mr. Eric Schwab, agronomist; Mr. Morris Welch, engineering technician, Mr. Dexter LaGrand, electronic technician; and Mr. John Walden, model maker.

Thanks are also due to my beautiful wife Stacy and my children Danté, Shyrell, Janoah, Christian, Journey, and the twins Willie and Clifford III, who supported and encouraged me through my academic pursuits.

Style manual or journal used Journal of Approximation Theory (together with the style known as "aums"). Bibliography follows IEEE Transactions Reference Style

Computer software used The document preparation package TEX (specifically LATEX) together with the departmental style-file `aums.sty`, MATLAB and LabVIEW.

Table of Contents

List of Figures x

1 Background and Literature Review 1
1.1 What Are Hardpans and How Are They Formed? 1
1.2 How Hardpans Affect Crop Production 1
1.3 Remediation 2
1.4 Vertical Soil Strength Measurement Devices 4
1.4.1 Cone Penetrometers 4
1.4.2 Multiple-Probe Cone Penetrometers 6
1.4.3 The Shortcomings of Vertical Soil Strength Measurement Tools 8
1.5 Horizontal Soil Strength Measurement Devices 9
1.5.1 Single-Depth Horizontal Soil Strength Measurement Devices . 10
1.5.2 Three-Depth Soil Strength Measurement Devices 13
1.5.3 Soil Strength Measurement Devices That Measure More Than Three Depths 15
1.6 Introduction of the On-The-Go Soil Strength Sensor 19

2 Control System Modeling 21
2.1 Introduction 21
2.1.1 Typical Motion Profiles 21
2.2 Description of proposed hardware 23
2.3 Model description 24
2.3.1 Modeling the sensors and other signals 24
2.3.2 Modeling the valve characteristic 27
2.3.3 Modeling the hydraulic system 27
2.4 Simulation Results 28
2.4.1 Step Response 28
2.4.2 Deadband 30
2.4.3 Sinusoidal response 33
2.4.4 Sinusoidal and Chirp input 33
2.4.5 The plot 38
2.5 Conclusions 39

3 Control System Design and Implementation 41
3.1 Introduction . . . 41
3.2 The Block Diagram Flow . . . 41
3.3 Command Signal Output . . . 42
3.3.1 DGPS to Calculate Oscillation Frequency . . . 42
3.3.2 Command Voltage . . . 44
3.3.3 System Startup and Configuration . . . 47
3.3.4 Operation Mode . . . 52
3.4 Deadband Compensation . . . 53

4 Experimental Evaluation 56
4.1 Experimental Approach . . . 56
4.1.1 Step Response Tests . . . 58
4.1.2 Plant Frequency Response . . . 60
4.1.3 PID Controller Response . . . 60
4.1.4 Closed Loop Response . . . 60
4.1.5 OSSS In The Field . . . 63

5 Conclusions and Future Work 65
5.1 Summary . . . 65
5.2 Future Work . . . 65

Appendices 67

A The Printed Circuit Board 68
A.1 37 Pin Connector . . . 68
A.2 9 Pin Connector . . . 68

B The Frame 72

Bibliography 75

List of Figures

1.1 Diagram of hand-held soil cone penetrometer used to measure the depth and degree of soil compaction. [1] 5

1.2 Side and front view of multiple-probe soil cone penetrometer created to expedite the measurement of soil compaction across a row and throughout a field [2] 7

1.3 Horizontal tip penetrometer probes. The items in the photo are (1) cone tip, (2) cone rod, (3) cone blade, (4) prismatic tip, (5) prismatic rod, (6) prismatic blade, (7) carrier bolt, (8) load cell, (9) I/O cable, (10) load cell housing, (11) housing bolt, (12) nut, and (13) cable protector [3] 11

1.4 Acoustic compaction layer detection device. Tine design (A) with a cone (B) and a microphone (C) [4] 12

1.5 Schematic of the vertical smooth blade (edge is on the left side) [5] . 14

1.6 Instrumented Subsoiler [6] 15

1.7 The three-depth soil mechanical impedance sensor designed by Chukwu and Bowers [7] 16

1.8 Operational concept of the soil strength profile sensor (OTG-SSPS): [8] 17

1.9 Profile Sensor mounted on a tractor [9] 18

2.1 The OSSS cycles once for every two segments. Vertical white lines represent segments. 22

2.2 SIMULINK block diagram model of the OSSS 25

2.3 Plots of the step response. Blue line plot is of the system with deadband. The red (+) plot is of system with deadband compensation. Position as a result of two step functions. First step a time 0 from 0 volts to 10 volts and the second step function at time 20 seconds from 10 volts to 0 volts with valve delay. 29

2.4 Deadband compensation 31

2.5 Simulation signals 32

2.6 Normalized output position and normalized flow rate plotted together. The blue (+) is the response while the black line is the flow rate. . . . 35

2.7 Position as a result of the chirp signal. The input starts a 0.0 Hz and increases to 1.0 Hz. And full stroke. 36

2.8 Chirp signal from 0-3 Hz. And 20 cm stroke. 37

2.9 Measurement range given tractor speed and cycle rate. 39

2.10 Three dimensional plot of system limits 40

3.1 Block diagram of the control system 42

3.2 Flow Chart 43

3.3 Algorithm to collect RMC sentence 45

3.4 Algorithm to parse RMC in LabVIEW 46

3.5 Command signal calculator in LabVIEW 48

3.6 OSSS's user interface 50

3.7 System with factory set deadband compensation. The solid line shows the input to the system. The dotted line shows the output movement of the shank with no deadband compensation in the amplifier. 54

3.8 System with deadband compensation adjustment in place. The solid line shows the input to the system. The dotted line shows the output movement of the shank with deadband compensation in the amplifier. 55

4.1 OSSS Mechanics Attached to Tractor 57

4.2 $G(s)$ (Open Loop Magnitude Response) 58

4.3 $G(s)$ Open Loop response. 59

4.4 Closed loop frequency response (Simulated) 61
4.5 Closed loop frequency response (Measured) 62
4.6 Closed Loop Response (collected in the field) 64
A.1 Printed Circuit Board 69
B.1 Frame1 73
B.2 Frame2 74

Chapter 1

Background and Literature Review

1.1 What Are Hardpans and How Are They Formed?

A hardpan is a layer of soil that is more compact than the layers above and below it. Hardpans are subsets of soil compaction and make up a small portion of the soil profile. In structural engineering, soil compaction is essential to forming stable construction foundations [10]. However, soil compaction is a problem in agriculture because it reduces crop yield. Soil compaction is present in all soil and it reduces crop yield by inhibiting seedling emergence and root penetration. These areas of increased soil strength beneath the topsoil which are formed by either natural processes or vehicle traffic, and hinder proper moisture levels necessary for successful crop production [11].

1.2 How Hardpans Affect Crop Production

In [12], Wells et al reported that crop yields were reduced by 25%, 30%, and even 40% when soil compaction problems existed. Some of this reduction is due to root restriction. Plants need an adequate rooting environment for optimal crop production [13]. Hardpans have been known to prevent roots from penetrating to depths of soil that could sustain plants during periods of short-term drought [11].

Another way that soil compaction reduces crop yield is by limiting the essential elements. When soil is severely compacted, tightly packed soil particles affect soil moisture and soil air, which are essential for plant growth [13]. Pore-size distribution and increased soil strength are responsible for limitations of soil moisture and air content [4]. Lack of moisture and air causes a reduction in photosynthesis, thus reducing crop yields [13].

1.3 Remediation

To allow plant roots to penetrate to less compact, moister horizons, many producers rely on some form of deep tillage to break through the hardpan layer [11]. Because tilling beneath the hardpan will break up the compacted area and allow deeper rooting and improve plants' ability to withstand short-term drought, crops grown in tilled fields, where soil compaction was previously a problem, have a better chance to grow successfully [11].

Traditional tillage treatments have focused on preventive maintenance and have not had the benefit of diagnostic evidence [14]. Though hardpan properties vary in strength and depth due to management practices and soil and crop factors [4], most farmers uniformly till at the maximum depth of their tillage equipment [15]. However, studies have shown that the hardpan varies greatly in depth and strength from field to field, or from one area to another within a field [11], [4], [14].

Excessively deep tillage can waste energy, increase surface erosion and decrease crop yields due to excessive soil disturbance [11]. Changing the tillage depth according

to local soil conditions preserves soil ecology and saves energy [16]. In [15], Raper et al found that the necessary tillage power could be reduced by 27% with variable-depth tillage compared to uniform-depth tillage. Variable-depth tillage also caused less damage to cover crops, thereby increasing crop yields [15]. Therefore, it is clear that variable-depth tillage is necessary to optimize the resources used in the tillage process and maximize plant yields.

The inherent inefficiency of uniform tillage treatments has been recognized by researchers who proposed tillage systems where the hardpan depth itself prescribes the tillage treatment [14]. In other words, the tillage depth will be based on the hardpan depth [14]. This variable-depth subsoiling requires accurate determination of the hardpan layer depth to be conveyed to an actuation mechanism that controls the tillage depth [4]. Another option would be map-based variable-depth subsoiling, which can be realized with geo-referenced hardpan depth information [4].

Most tools currently used for variable hardpan detection can be classified as either vertical or horizontal measurement devices. The vertical and horizontal devices both have a force transducer to measure the soil penetration resistance as they move through the soil profile. The depth at which the necessary penetration force peaks is the hardpan depth (if a hardpan exists). The difference in the two types of tools can be explained by the ways in which they move through the soil profile.

1.4 Vertical Soil Strength Measurement Devices

Vertical devices sense the penetration resistance of soils and measure the force needed to push a cone tip into the soil vertically [14], [17]. As the probe is being forced into the ground, it encounters layers of various compaction intensities. The force necessary to penetrate each layer increases as the compactness or density of that soil layer increases.

Vertical devices have the benefit of continuous vertical measurements. With data collected with these devices, a continuous soil strength profile can be achieved in the vertical direction. The drawback of vertical devices is their stationary (in the lateral sense) data collection method. This stop-and-go method limits the measurement capabilities in the horizontal (lateral) directions and increases the time needed to survey a field.

1.4.1 Cone Penetrometers

One such vertical device is the cone penetrometer [1], which has traditionally been used to assess soil penetration resistance [14], [17]. The first penetrometers were hand-held tools like the one shown in Figure 1.1.

This tool has a load-measuring device in series with the shaft and handle. The load-measuring device, which is aligned with the shaft and handle, measures the force applied to the handle as the cone is pushed into the soil.

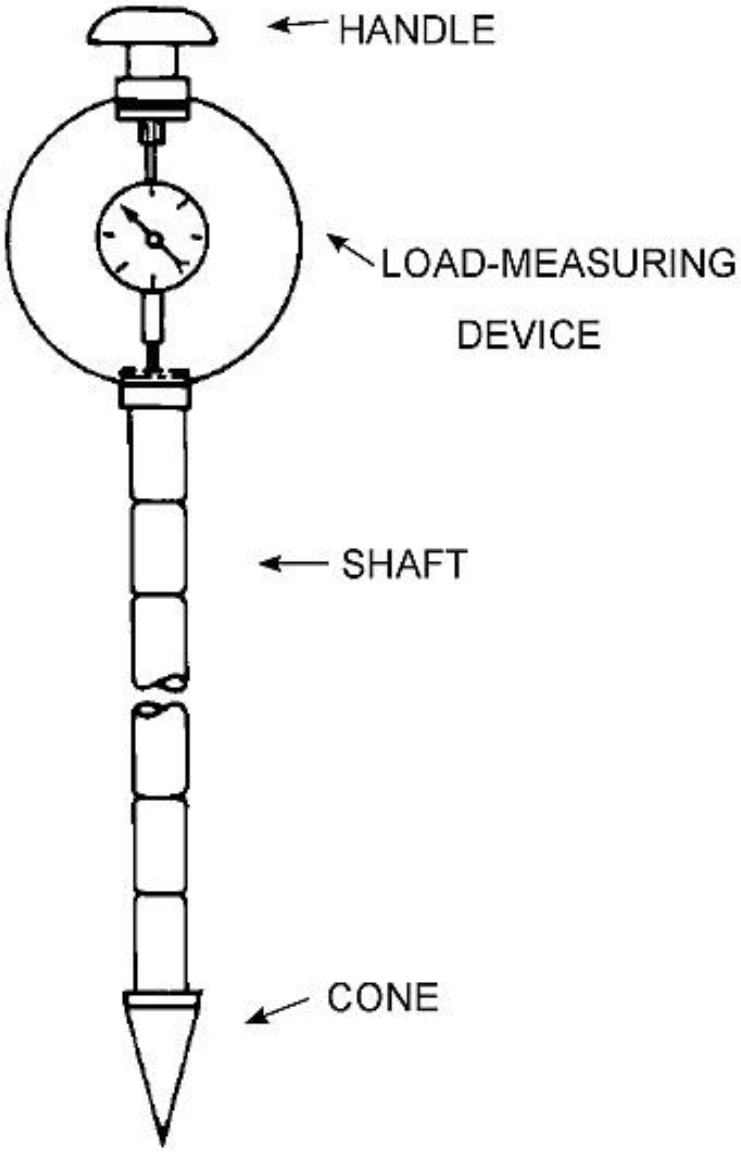

Figure 1.1: Diagram of hand-held soil cone penetrometer used to measure the depth and degree of soil compaction. [1]

Variations of cone penetrometers may have been used as early as the 1800's. Although it is not well documented, a needle-type penetrometer was used to estimate various types and consistencies of soil [17]. The Danish railroad companies used pocket penetrometers to determine maximum allowable bearing pressure in the 1930's [17]. In 1948 the U.S. Corps of Engineers developed hand-operated cone penetrometers for predicting trafficability of vehicles at the Waterways Experiment Station in Mississippi [17]. The first tractor-mounted penetrometer was designed and built by J. R. Williford, O. B. Wooten, and F. E. Fulgham in 1972. This penetrometer was mounted on rails that allowed its one probe to be moved from side to side [18]. An X-Y plot was constructed with the data collected.

1.4.2 Multiple-Probe Cone Penetrometers

Although soil cone penetrometers can determine soil strength and various levels of soil compaction, they are still not fast enough when surveying large fields, where several samples are needed. In one experiment it took three days to collect 800 sets of force-depth data using a single-probe device [2]. Some of the recently developed cone penetrometers have multiple probes (see Figure 1.2) that are forced into the soil simultaneously.

Adhering to the standards set forth by the American Society of Agricultural Engineers in 1993 (ASAE Standard S313.2), Raper et al developed a multi-probe soil cone penetrometer (MPSCP) containing five probes instead of one [2]. With this

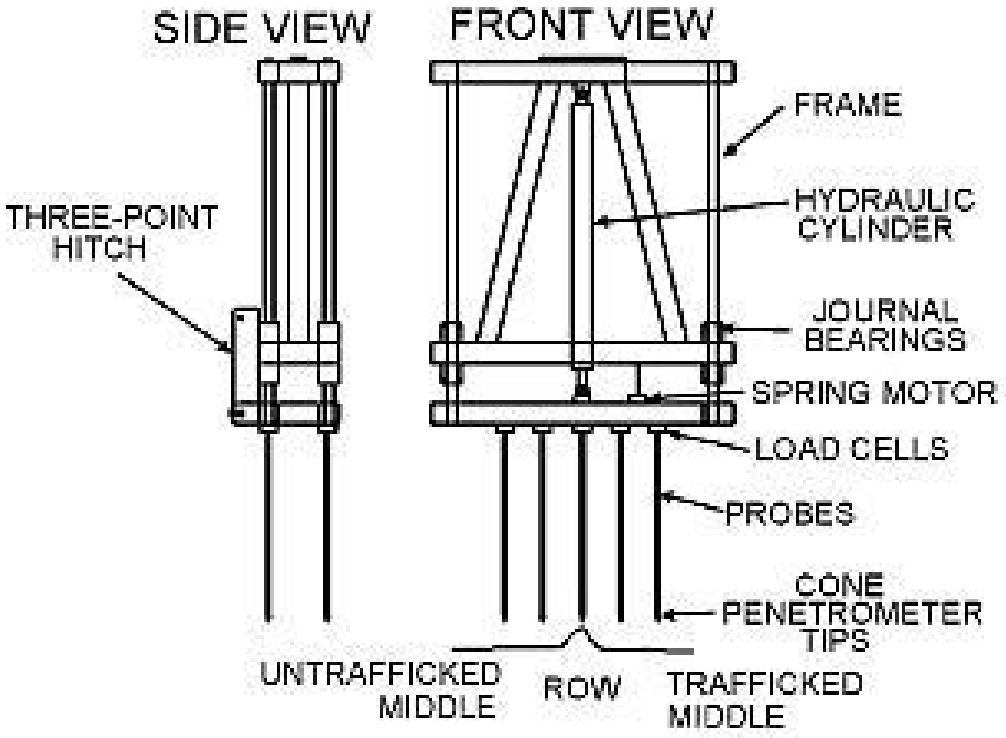

Figure 1.2: Side and front view of multiple-probe soil cone penetrometer created to expedite the measurement of soil compaction across a row and throughout a field [2]

MPSCP, the data from five positions across the row could be collected at one time, reducing the time necessary to collect data from a plot.

1.4.3 The Shortcomings of Vertical Soil Strength Measurement Tools

In large-scale field settings, the vertical cone penetrometer is an impractical method of determining soil compaction [14]. Multiple-probe cone penetrometers are faster than the single-probe penetrometers and are less labor-intensive, but they are still relatively slow. Another problem with this system is that the multiple-probe cone penetrometer, like the single-probe penetrometer, can only determine soil strength at discrete sampling points. This stop-and-go sampling procedure is hard to incorporate into a continuous variable-depth tillage practice [4] and maps interpolated from this point data are limited due to small measurement density [5]. Hand-held penetrometers like the one shown in Figure 1.1 have been found to be difficult to use if the soil contains very compact layers [19]. When the soil is compacted, the operator has trouble maintaining a constant speed when inserting the unit into the ground [19]. This is a problem because speed variations can influence the readings [19]. Machine-driven penetrometers use hydraulic fluid power to force the probe into the ground at a constant speed. However, this hydraulic power comes with bulky machinery and a tractor to supply the fluid flow. Horizontal devices would have comparable hydraulic machinery but would require less time to collect data compared to vertical penetrometers.

1.5 Horizontal Soil Strength Measurement Devices

Several attempts have been made to develop horizontal cone index measurement devices. Horizontal devices measure the force needed to push a wedge tip through the soil horizontally. As the probe is being pulled or pushed through the soil, it will encounter differences in soil mechanical impedance [20]. The mechanical impedance increases as the compactness of the soil increases. Unlike the vertical devices, the horizontal devices are designed to be inserted into the soil and pulled. This method of soil strength measurement eliminates the stop-and-go drawbacks of the vertical system, but unfortunately presents disadvantages of its own.

Horizontal devices have the benefit of continuous horizontal measurements. With the data collected with horizontal devices, a continuous soil strength profile can be achieved in the horizontal direction. Horizontal or on-the-go soil mechanical resistance measurements allow substantial increase in measurement density and speed [16]. The disadvantage of horizontal devices is their constant depth measurement limitations. The depth of measurement remains constant while the hardpan depth is varying throughout the field. Because the soil strength profile is measured for only certain depths, it is possible to incorrectly measure the hardpan location. Many of these devices are discussed subsequently.

1.5.1 Single-Depth Horizontal Soil Strength Measurement Devices

Horizontal Blade Penetrometers

Alihamsyah and Humphries built a tool capable of rapid soil strength determination at one depth [14]. This tool (seen in Figure 1.3) uses a prismatic tip penetrometer attached to a force transducer [8].

Alihamsyah et al developed and tested this device in 1990 and found that this horizontal penetrometer could serve as soil impedance measurement device [3]. Alihamsyah proposed the idea of mounting a horizontally operating soil strength measuring tip near the front of a tractor providing soil physical data to a microcomputer [3]. This system could be an integral part of a control system that would adjust tillage equipment automatically [3].

Acoustic Compaction Layer Detection

M. Tekeste, a research graduate student assistant at the University of Georgia, developed an acoustic system that could be used as an on-the-go hardpan detection device [4]. This acoustic compaction layer detection device (ACLDD) (seen in Figure 1.4) measures the sound level as it is drawn through the soil at different depths [4].

Figure 1.4 shows that this acoustic tool has a design similar to horizontal measurement tools. The difference between the ACLDD and the other horizontal devices is that a sound transducer is employed instead of a force transducer. Tekeste's hypothesis was that the sound level would be proportional to soil compactness. The

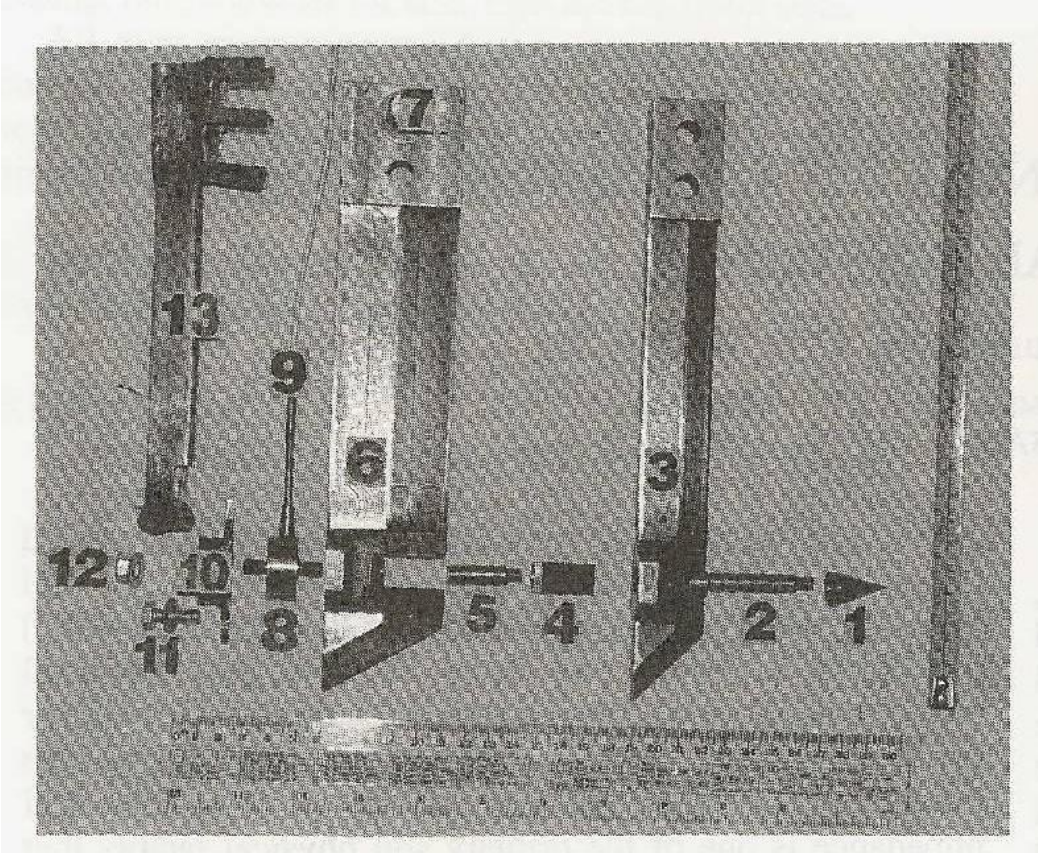

Figure 1.3: Horizontal tip penetrometer probes. The items in the photo are (1) cone tip, (2) cone rod, (3) cone blade, (4) prismatic tip, (5) prismatic rod, (6) prismatic blade, (7) carrier bolt, (8) load cell, (9) I/O cable, (10) load cell housing, (11) housing bolt, (12) nut, and (13) cable protector [3]

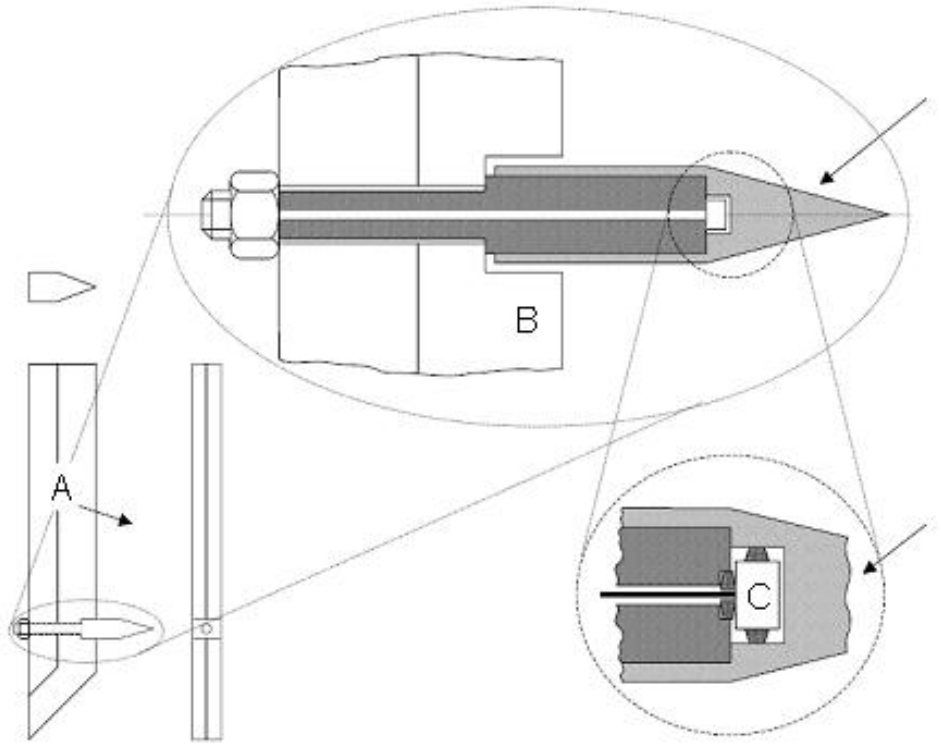

Figure 1.4: Acoustic compaction layer detection device. Tine design (A) with a cone (B) and a microphone (C) [4]

sound recorded by the system would be of higher amplitude when the microphone was being pulled through more compact soil.[4]. The ACLDD is capable of detecting the soil compaction layer effectively and inexpensively [4].

1.5.2 Three-Depth Soil Strength Measurement Devices

Strain gauge array

Adamchuk designed and tested a vertical smooth blade (VSB) device to dynamically measure soil penetration resistance at three depths [5] (see Figure 1.5).

This device consists of a tapered cantilevered beam with an array of strain gauges that cut through the soil [5]. The varying soil resistances cause deformations in the beam that are detected by the strain gauges [5]. The available measurement depths would be "p1", "p2", and "p3", as seen in Figure 1.5.

Instrumented Subsoiler

Manor et al developed an instrumented subsoiler to map hardpans [6]. This device, shown in Figure 1.6 is also capable of soil strength measurements at three depths.

This system works with three load cells and a potentiometric sensor that measures the resultant direction and magnitude of the forces acting on the shank [6]. The resultant forces would be different depending on its depth relative to the hardpan [6]. This system has the hydraulic actuator so that the depth can be adjusted.

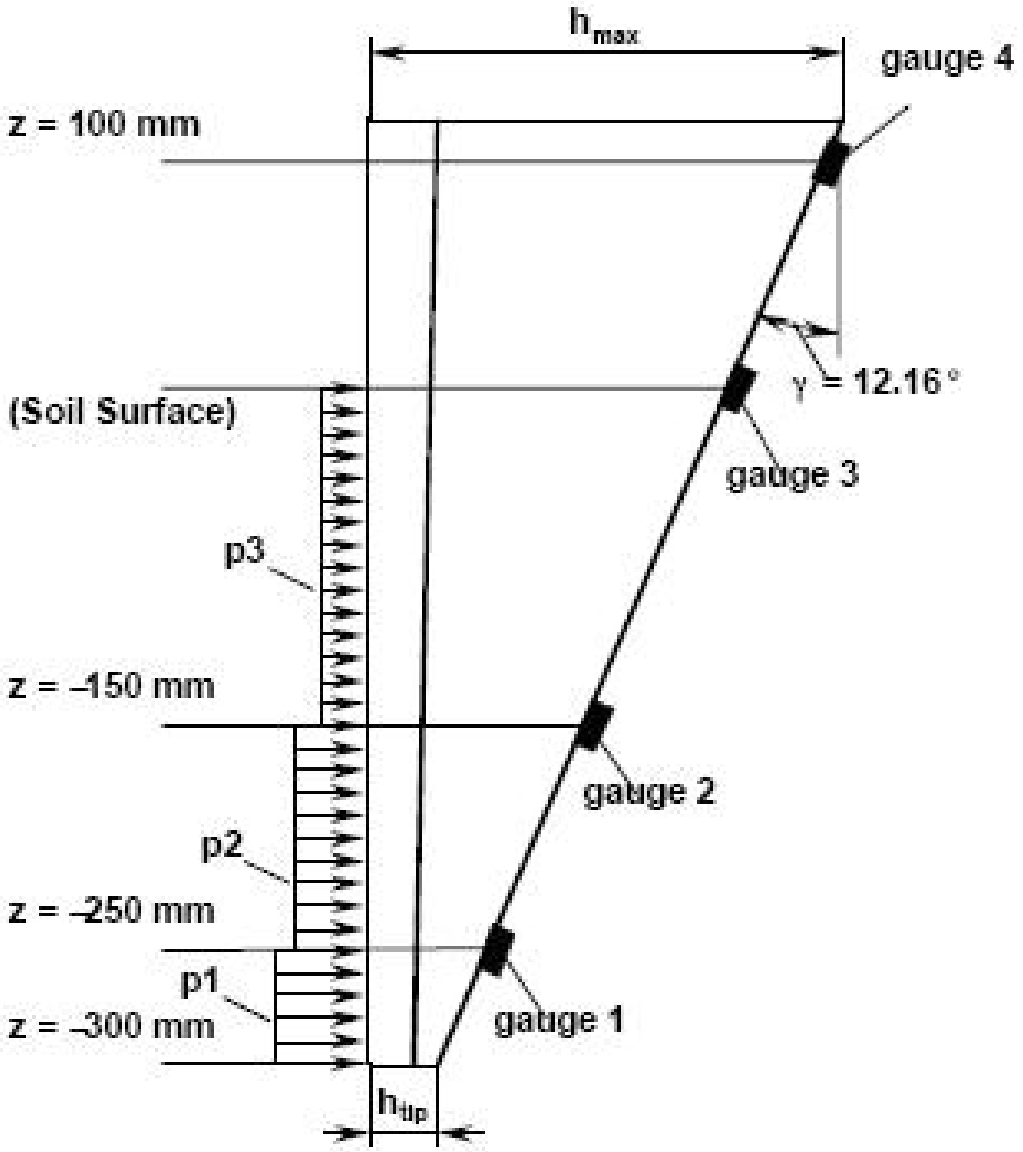

Figure 1.5: Schematic of the vertical smooth blade (edge is on the left side) [5]

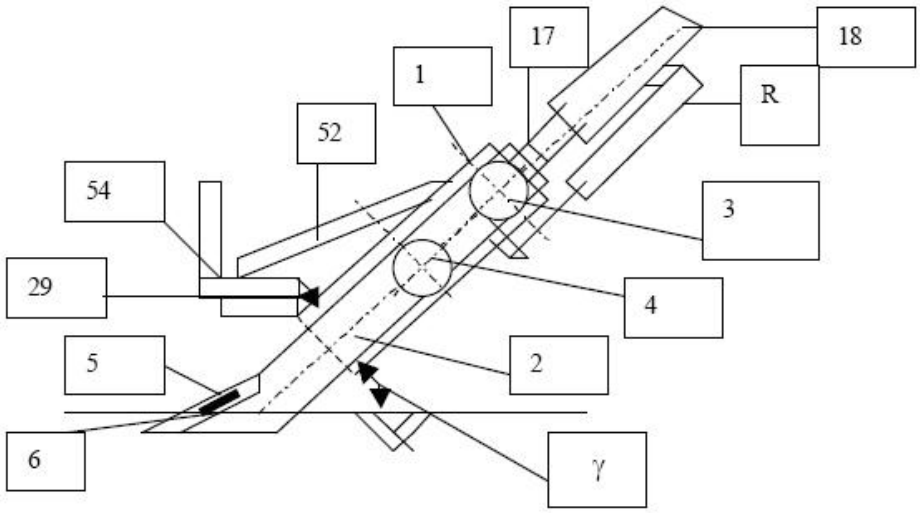

Figure 1.6: Instrumented Subsoiler [6]

Instantaneous Multiple-Depth Sensor

Chukwu and Bowers developed a three-depth continuous soil mechanical impedance sensor (seen in Figure 1.7) [7]. This design uses three load cells mounted on a blade carrier. These load cells measure the force applied to the penetrometer tips [7].

1.5.3 Soil Strength Measurement Devices That Measure More Than Three Depths

Load Cell Array

S. O. Chung et al developed an on-the-go soil strength profile sensor using the load cell array (OTG-SSPS). This device, seen in Figure 1.8 is capable of measuring soil strength at five depths. This device consisted of multiple sensing tips attached

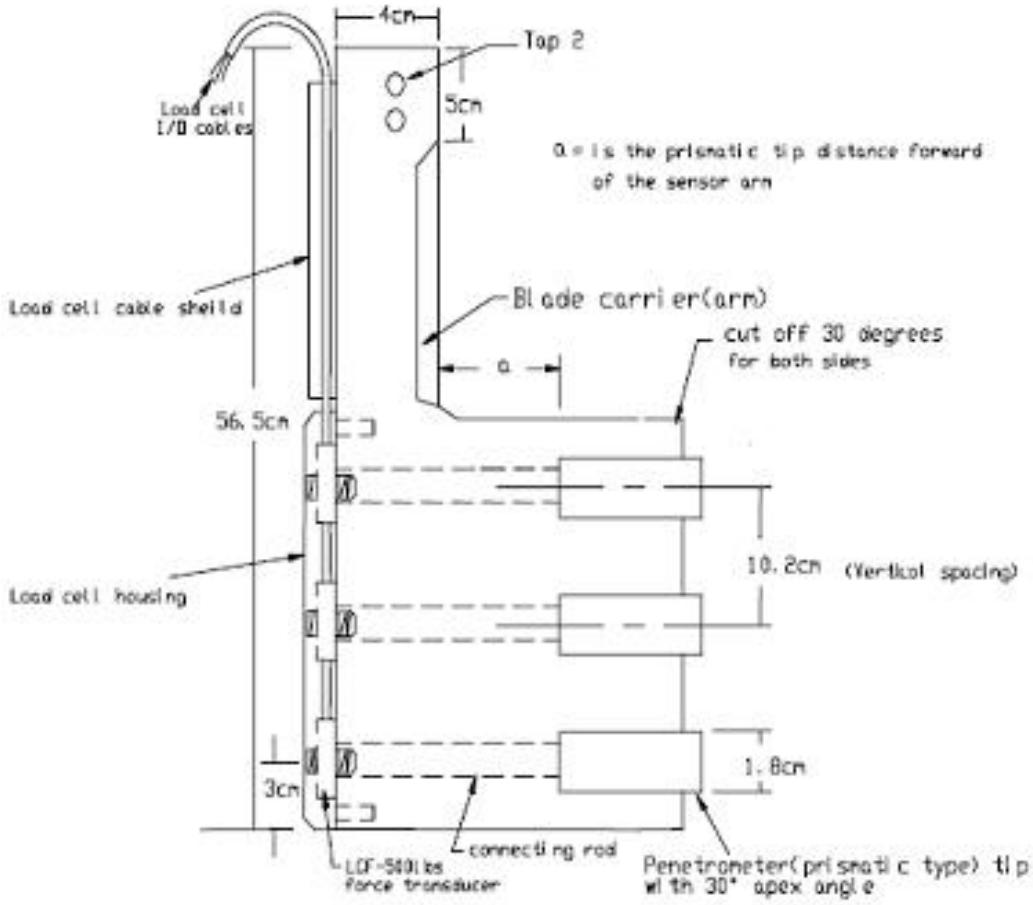

Figure 1.7: The three-depth soil mechanical impedance sensor designed by Chukwu and Bowers [7]

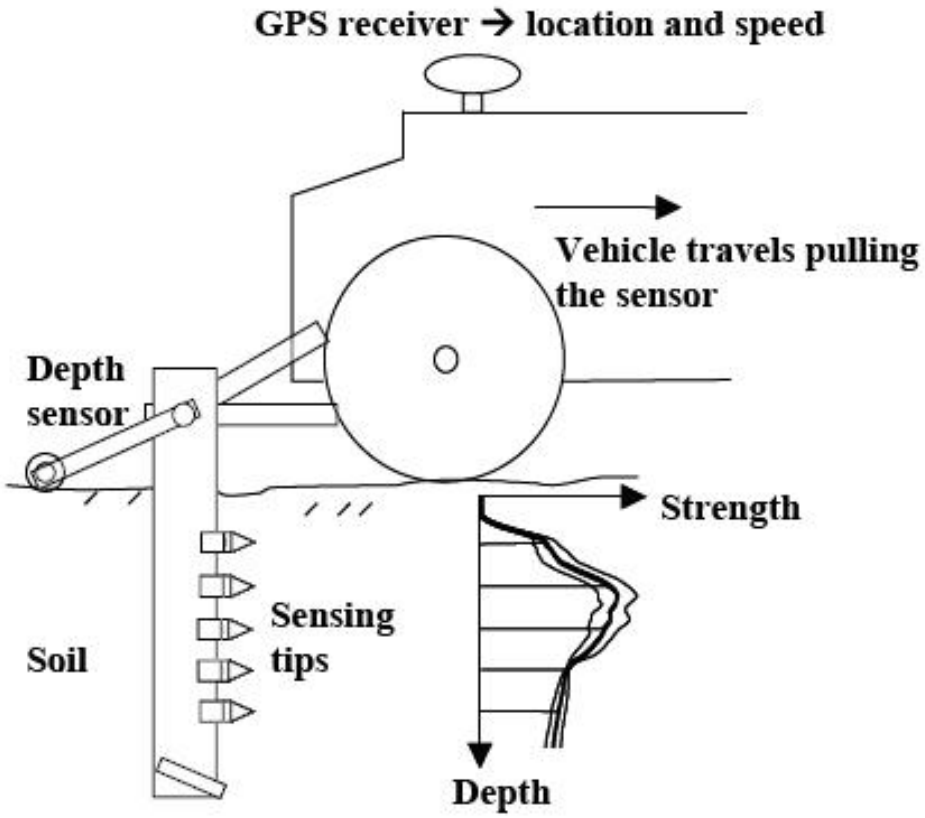

Figure 1.8: Operational concept of the soil strength profile sensor (OTG-SSPS): [8]

to load cells. Each sensing tip gives a soil strength measurement. The OTG-SSPS obtained continuous "cone index like" measurements at discrete depths as it was pulled through the soil [8].

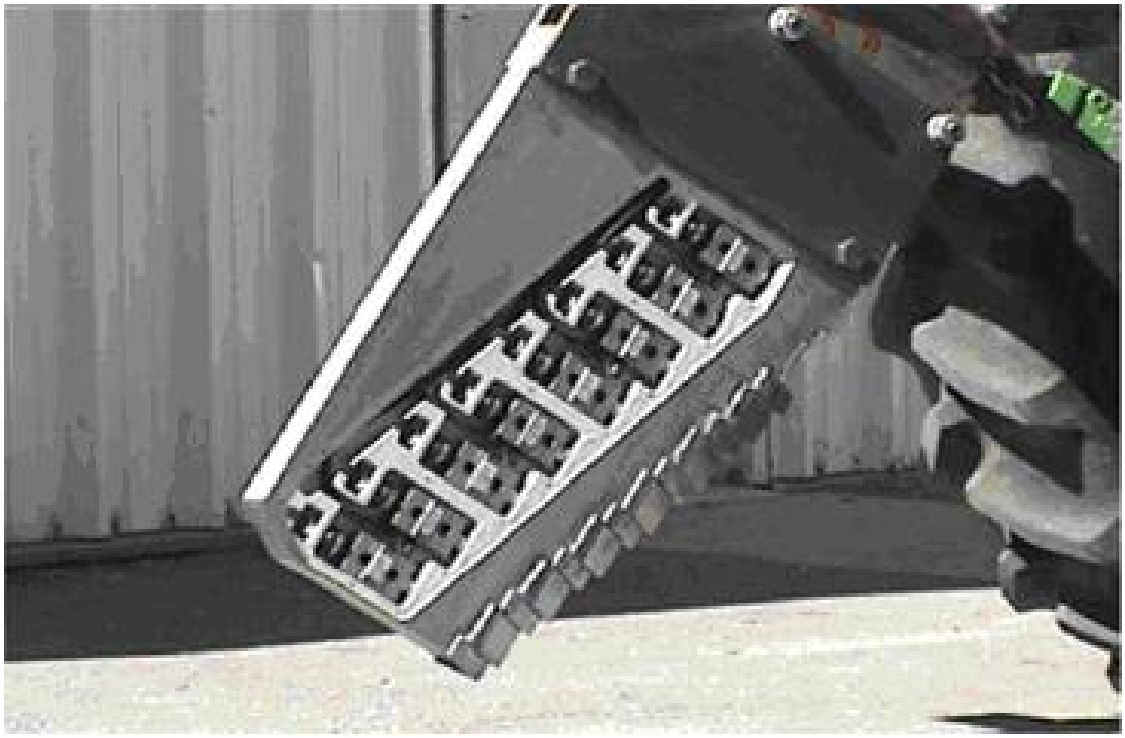

Figure 1.9: Profile Sensor mounted on a tractor [9]

Profile Sensor

P. Andrade et al developed a profile sensor (PS) which consisted of eight cutting edges supported by load cells [21]. This device, seen in Figure 1.9, was designed to provide information on soil resistance at eight depths [21].

The PS measures forces on load cells located inside the shank [9]. Based on the instrumented tine developed by Glancey et al, [22] and the texture/compaction index (TCI) , the profile sensor measures force on the eight cutting edges as the tine is pulled through the soil [21].

All of these horizontal strength measurement devices are capable of hardpan detection at multiple, different depths but they all have one inherent shortcoming. Their common flaw is their discrete depth measurement [14]. These tools are designed to be inserted in the soil and pulled at a constant depth. Therefore, the measurement depths are constant while the hardpan depth is not. When the actual hardpan depth is different from the sensor depth, erroneous or missing soil compaction depth measurements become a problem [14]. If the placement of the sensors is not close enough to the hardpan, it could go undetected as it would fall between two sensors [14]. In other words, the sensor must make contact with hardpan to give correct measurements. If the sensor does not make contact, the hardpan remains undetected.

1.6 Introduction of the On-The-Go Soil Strength Sensor

Vertical penetrometers are capable of continuous vertical cone index measurement but they are limited to discrete horizontal (across the field) samples. The horizontal penetrometers studied to date are capable of continuous horizontal cone index measurements but are limited to discrete vertical depth measurements. E. Hall and R. Raper proposed the idea of an on-the-go horizontal soil strength measurement system that oscillates vertically as it is pulled through the soil[14]. With this device, continuous depth soil cone index measurements can be achieved by using a single vertically oscillating sensor [14]. Like the other horizontal soil strength measurement devices, the On-The-Go Soil Strength Sensor (OSSS) includes a downwardly extending shank with a sensing tip mounted on the leading edge [23]. The difference

between this device and the other horizontal soil strength measurement devices is its reciprocating motion. This horizontal motion would allow continuous variable-depth soil strength profile measurements over a large area [23]. The reciprocation motion of the OSSS works similarly to a sewing machine. The hydraulic valve (motor) controls the shank's (needle's) vertical movement. The ground (fabric) moves horizontally relative to the shank. This motion causes the sensor (eye) to move through the soil in a sinusoidal motion. The horizontal motion of the device being pulled through the soil combined with a vertical oscillation enables a continuous sinusoidal (vertical and horizontal) measurement of the mechanical impedance throughout the profile [20].

The OSSS concept was tested in the soil bins at the USDA National Soil Dynamics Laboratory at Auburn University in Auburn, Alabama. The current need of the OSSS project is to design and develop the automatic control system and hardware. The control system serves as the brains of the system and controls the shank oscillation. The hardware of the system consists of the tool bar on which the OSSS rests, the hydraulic system that powers the OSSS, and the electrical components for signal conditioning. With the development of the control system and hardware components, the work of E. Hall and R. Raper can come to fruition.

Chapter 2

Control System Modeling

2.1 Introduction

The speed and range of the On-the-fly Soil Strength Sensor (OSSS) data collecting capabilities are limited by the hydraulic system (particularly the slew rate of the rod extension) that actuates its motion. However, the OSSS operator would need to transverse the path at a reasonable speed and collect sufficient data to determine hardpan depths thoroughly throughout the field. To assist with determining the limits of speed at which the operator can travel and collect data, a system model and simulation are studied using MATLAB & SIMULINK.

2.1.1 Typical Motion Profiles

Figure 2.1 shows a diagram of how the OSSS should oscillate. The space between the white vertical lines is the distance for each soil strength profile. If the distance between the white lines is 10 meters then the cycle rate is 10 m per cycle. The large amplitude sinusoidal line is the vertical position of the soil strength sensor when the OSSS is pulled through the soil. The semi-straight horizontal line in the middle represents the hardpan.

A LabVIEW software program controls a power amplifier which, in turn, drives the proportional directional valve to produce the vertical oscillation of the tine. The

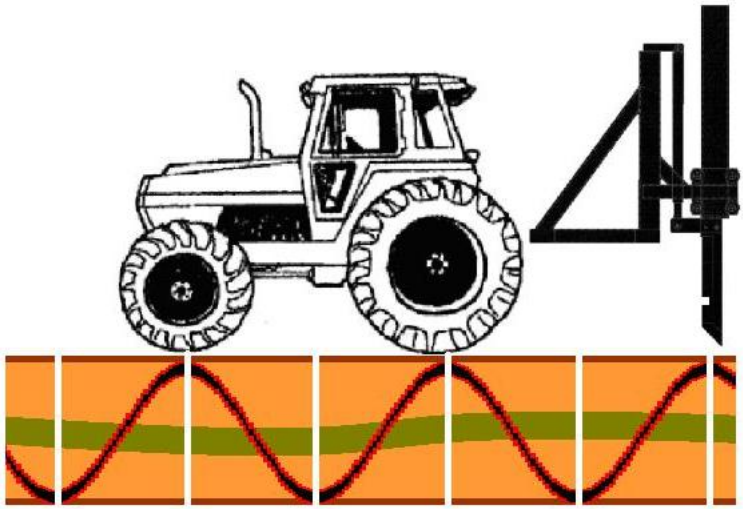

Figure 2.1: The OSSS cycles once for every two segments. Vertical white lines represent segments.

tine is set to cycle at specified horizontal distances (e.g. 15 horizontal feet per cycle) regardless of the tractor speed. If the tractor travels too fast, a sinusoidal motion with the desired amplitude is unachievable. One method to achieve increased tractor speed would be to restrict the depth range to those depths that might actually contain the hardpan instead of allowing the full range of the hydraulic cylinder to be used. For example, peaks in soil strength typically occur at depths approximately 20-40 *cm* beneath the soil surface [11]. Therefore, the measurements could be restricted to this range. This smaller oscillation range would allow the system to cycle faster. However, restricting the measurements to the hardpan would ignore deeper rooting restrictions that could be 50 *cm* or deeper.

Another option could be to extend the cycle distance. The problem with this approach is the tremendous variation in site-specific hardpan depth. Using descriptive semivariogram statistics, Raper et al [11] found variations in the depth to hardpan as close as 12.4 m in some Southern U.S. fields. Therefore, if the cycle rate is too low, a good map of the hardpan can not be created from the data. What is needed is a three-dimensional plot of speed versus cycle rate versus cycle range that would allow one to determine the limits of the system.

2.2 Description of proposed hardware

The OSSS unit consists of three components: a sensing tip, a shank, and a force transducer. The OSSS shank was designed to provide a method of inserting the force transducer and the soil strength sensing tips into the soil. The shank was designed to be pulled at a perpendicular rake angle to the soil surface at a maximum effective measuring depth of 600 mm.

The control program was written in LabVIEW [1] to control the cycle rate and range with a command signal realized by National Instrument data acquisition card (model DAQ 6025E). This data acquisition card is capable of producing a 10 volt analog signal which is amplified by the PID module (Vickers model EEA-PAM-561-D-32).

GPS navigation is used to calculate the tractor speed as well as the geographical position of the tine. A depth sensor measures the relative distance of the OSSS to the

[1] LabVIEW is a product of National Instruments

soil surface and a draw-wire displacement sensor (Micro-Epsilon model WDS-Z100) measures the position of the oscillating tine relative to the OSSS frame. The force transducer that measures the tillage force necessary to push the OSSS through the soil is the SENSOTEC®[2] GR3 load beam (SENSOTEC®, Columbus, Ohio 43228), with a 4.45-kN measurement capacity. The GR3 load beam is a cantilever beam design, capable of measuring tensile and compressive loads. The information from the force transducer is stored with the DGPS (Differential Global Positioning System) data in a form that can be used to draw 3D maps of the hardpan for the entire field post data collection.

2.3 Model description

To ensure that the system could perform as needed, a model was constructed in SIMULINK (see Figure 2.2).

2.3.1 Modeling the sensors and other signals

The "Draw-Wire Sensor" block in Figure 2.2 was modeled as a gain block with the minimum displacement of the stroke being 0 volts and the fully extended stroke represented as 10 volts. This sensor has a gain of 9.4 v/m and is used to measure the actual extension of the rod. Moving clockwise around the diagram, there is

[2]Use of company names or trade names does not imply endorsement by USDA-ARS or Auburn University.

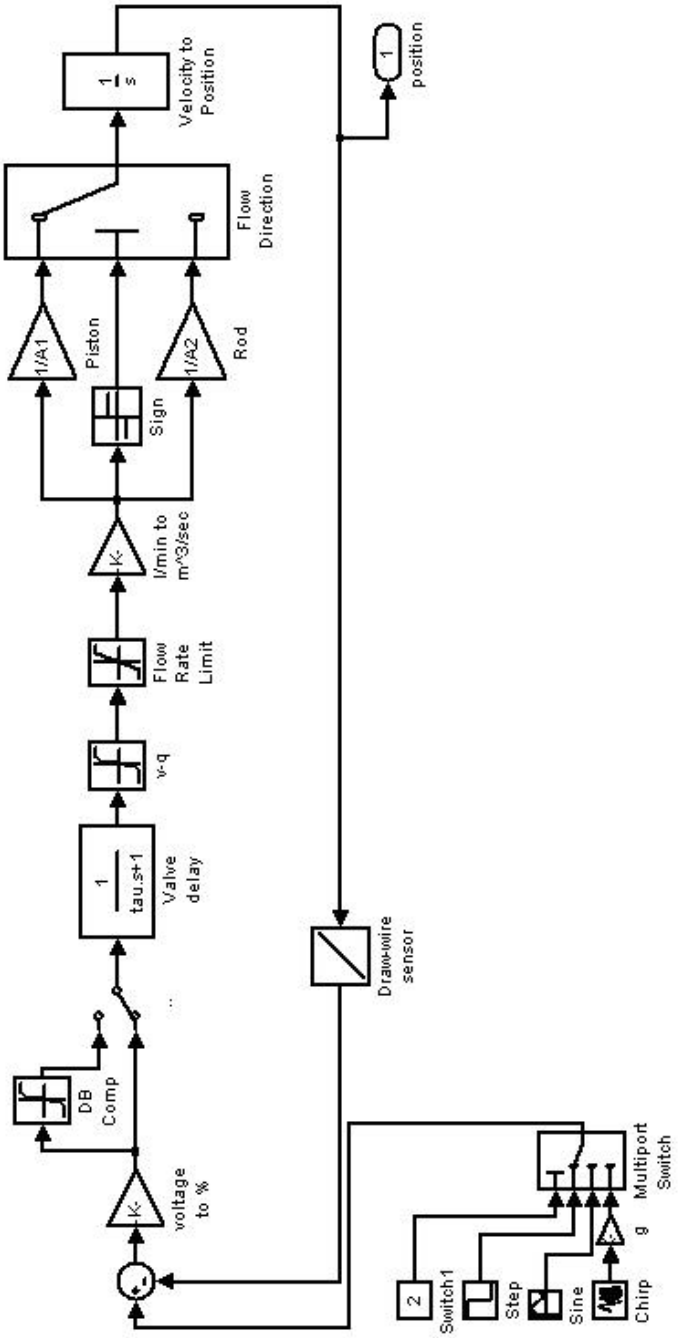

Figure 2.2: SIMULINK block diagram model of the OSSS

the summing junction, which represents subtracting the voltage of the displacement sensor from the command signal; the difference is the error signal.

The command signal may be modeled as a sine wave, a chirp (frequency increasing over time) signal, or a step function. The sine wave has adjustable amplitude and frequency that are calculated from the parameters in a separate MATLAB m-file. The parameters used to determine the amplitude and frequency of the sine wave are the measurement range and the tractor speed cycle rate ratio, respectively. The chirp signal is a sinusoidal wave with amplitude equal to 1 and a frequency that increases over time. The amplitude of the chirp signal is scaled up and biased so that the output is 0-10 volts. The step function consists of two steps. The first step at time 0 s is from 0 volts to 10 volts and the second step at time 10 s is from 10 volts to 0 volts. This choice of input signal is made with a "Multi-port Switch" block.

The reference manual used "percent of voltage" instead of voltage in the command signal to flow rate chart [24]. Therefore, the error signal is converted to a percent of command signal using a gain block labeled "voltage to %" such that 100% represents 10 volts. A choice is made whether the error signal is deadband compensated or not with a manual "switch" in the simulation diagram. This conditioned error signal flows to the block labeled "Valve Delay". Valve characteristics are discussed below.

2.3.2 Modeling the valve characteristic

The "Valve Delay" block represents the inherent delay characteristics of the solenoid within the valve. The controller output (control signal) goes through a look up table, where it is converted to a fluid flow rate (q). A lookup table for the command signal versus flow rate was tabulated from the information given in the valve manual (Vickers model GB-C-2007C). A graph digitizer was used to sample the valve characteristic curve - these samples were not uniformly spaced, so linear interpolation is not straightforward. Then, the non-uniformly sampled table was converted to an equation using the Microsoft Excel trend line function. The equation was finally converted to a lookup table of uniformly spaced values in the MATLAB m-file. The lookup table labeled "v-q" converts the control signal percentage to flow rate.

2.3.3 Modeling the hydraulic system

The tractor hydraulic flow rate of the John Deere 6410 is limited to 113 l/m (30 g/m) and this limit is seen next in the block labeled "Flow Rate Limit." The units of flow rate are converted to m^3/s. Flow rate divided by the area of the cylinder (m^2) yields the rod velocity (m/s).

A hydraulic cylinder with a 6.35 cm (2.5 in) bore, a 3.493 cm (1.375 in) piston and a 106.68 cm (42 in) stroke was used for model. These cylinder dimensions are of the Chief model WP #286-242 which is used on the OSSS. The rod and piston areas are modeled in two separate gain blocks labeled "Rod" and "Piston." The sign

of the fluid flow triggers a switch that directs flow through the piston gain block or the rod gain block. The output of the "Flow Direction" block is the velocity of the rod actuation. This velocity is integrated over time in the integrator block labeled "Velocity to Position" to give rod position. The rod position is graphed in the scope labeled "Position".

2.4 Simulation Results

2.4.1 Step Response

The response of the rod as a result of a step function is shown in Figure 2.3. Ideally, the 10 volt signal would produce maximum extension. The time to extend the rod fully could be calculated with the basic hydraulic equation 2.1.

$$t = \frac{l}{v} = \frac{l}{\frac{q}{a}} \tag{2.1}$$

where v is velocity of the extending rod, q is fluid flow rate, a is cylinder area, t is time, and l is stroke length. This equation does not, however, take into account the deadband or the valve delay. In the SIMULINK model, the deadband and the valve delay (see Equation 2.2) are accounted for, thus allowing a better determination of the actual time the system takes to complete one cycle.

$$ValveDelay = \frac{1}{[tau, 1]} \tag{2.2}$$

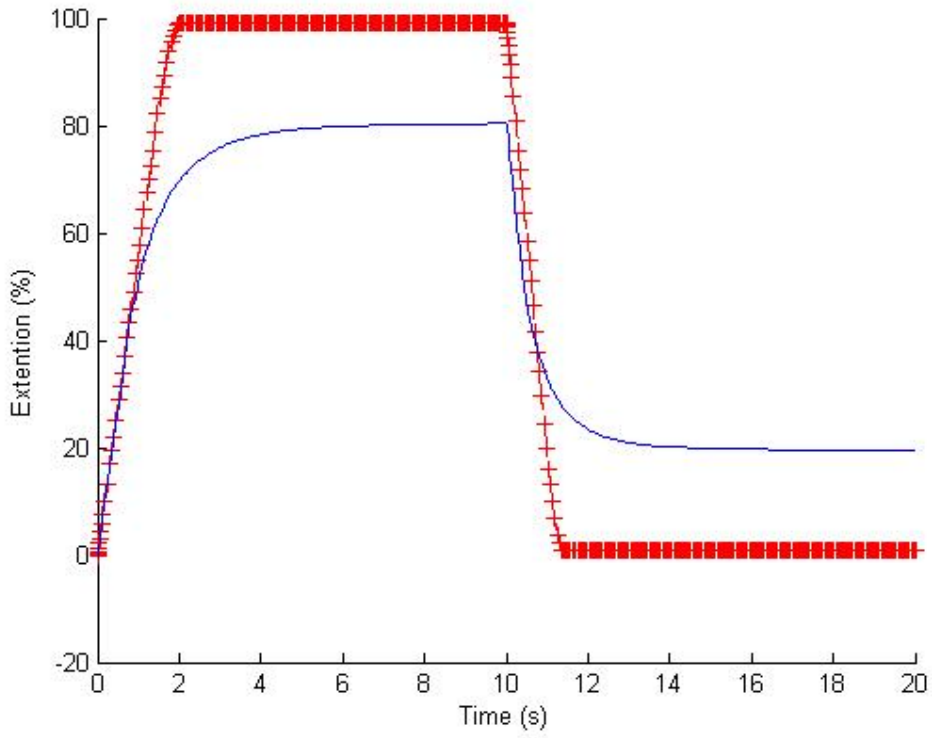

Figure 2.3: Plots of the step response. Blue line plot is of the system with deadband. The red (+) plot is of system with deadband compensation. Position as a result of two step functions. First step a time 0 from 0 volts to 10 volts and the second step function at time 20 seconds from 10 volts to 0 volts with valve delay.

Figure 2.3 shows the response of the system with unity gain and the step function input as described above. This figure shows the system response with no deadband affect in the red "+" plot. The effects of the deadband are shown in the blue line plot. With a step from 0 to 10 volts we would like to see the rod position extend from 0 to 100%. This is not the case with the blue line plot because of the deadband.

2.4.2 Deadband

A plot of the command signal to flow rate chart is shown in Figure 2.4 represented by the solid blue line. The flat region of this plot is the deadband. The deadband is the range of control signal that will produce a flow rate of zero. This deadband is useful in systems with appreciable noise because it will prevent noise induced movement of the actuator. However, because valve deadband is evident with small signals, the dead zone affects the system negatively when short rod movements are desired. In fact, rod motion halts whenever the control signal is too small, since the commanded control effort falls inside the valve deadband. In the simulation plot in Figure 2.5 it can be seen that a deadband compensator would improve the response.

There is a compensator onboard the amplifier that can be adjusted with a potentiometer. However, since the onboard compensator should not reduce the valve deadband to zero (because of noise), there will still be a dead zone. This dead zone is considerably smaller than the blue line plot in Figure 2.4. To further improve the system's small signal response a compensator was programmed in the control software. This compensator will adjust the output signal of the DAQ card causing the command signal to "hop" over the deadband region. The only time the command signal will be found in the dead zone is when the desired movement of the cylinder is zero. Then the command signal and the flow rate will be zero. A plot of the compensated signal is shown in Figure 2.4 represented by the red (+) line.

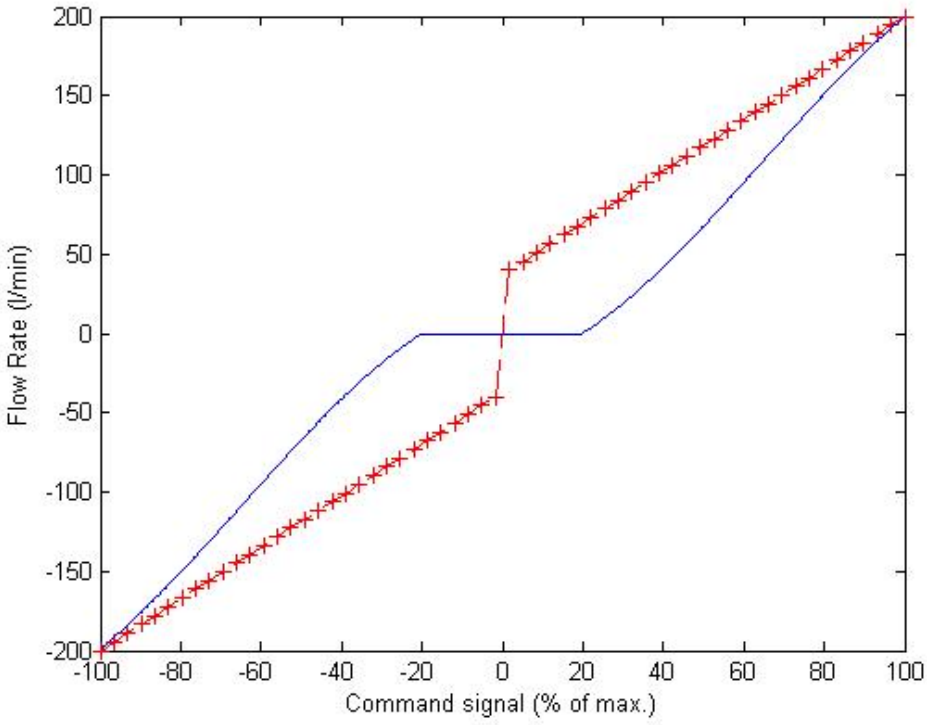

Figure 2.4: Deadband compensation

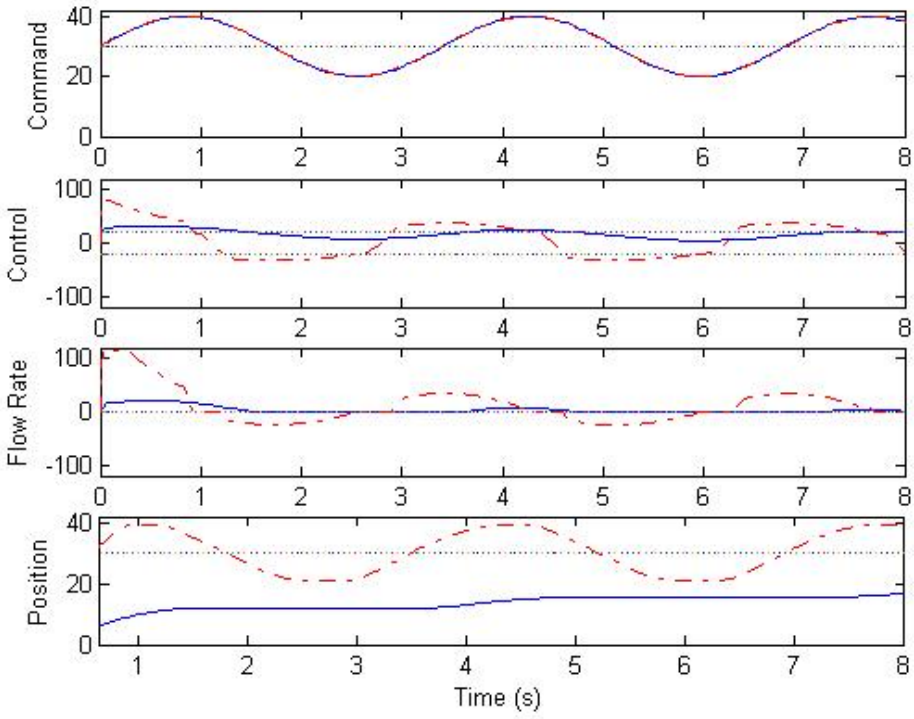

Figure 2.5: Simulation signals

2.4.3 Sinusoidal response

Figure 2.5 consists of four graphs: command (input) signal; conditioned error signal; flow rate; and rod position. Each graph consists of two plots. The blue (solid) line shows the effects of the deadband while the red/dashed line shows a deadband compensated system. The input signal is the same for both the compensated and the uncompensated system. For the sake of simplification the input signal is scaled up to represent the desired range of motion (20-40cm). With the uncompensated system (graph B blue/solid line) it is seen that the signal controlling the flow rate is in the deadband region most of the time. Graph "C" (blue/solid) shows that while our control signal is in the deadband range there is no flow to the rod. And the effects of no flow can be seen in graph "D" (blue/solid) as the position of the rod is unchanged. As a result, the rod will not oscillate. The blue lines in the figure show the system with deadband compensation. Graph "B" shows that the control signal skips over the deadband region. As a result there is flow to the cylinder when small movement is needed. Therefore the cylinder oscillates in small measurement ranges as seen in graph "D". It is concluded that deadband compensation is not only feasible but necessary since the 20-40 cm region is the primary [3] region.

2.4.4 Sinusoidal and Chirp input

The cylinder diameter and tractor flow rate limit are issues at high frequency oscillations. Simulation plots reveal when the upper limits are reached: the system

[3]The primary region is where the hardpan is found.

is unable to keep up. And the response plot takes on a triangular wave form. Figure 2.6 shows this "clipping." In this figure the flow rate and the response are normalized and plotted together. The blue/plus line is the response and the black line is the flow rate. It can be seen that the flow rate is maxed out while the rod is actuated and then crosses zero when the rod actuation direction changes. Because the velocity of the collapsing rod is greater than the extension velocity the sinusoidal motion is seen at the lower part of the plot. When the rod reaches 100% and changes direction a triangle shape is seen because the cylinder never reaches 100% extension. In other words the higher the oscillation frequency the lower the ability of the system to keep up.

With a chirp signal input the limits of the oscillation frequency at a certain measurement range can be explored. Another way of stating this is how fast the tractor can travel since the oscillation frequency is directly proportional to the tractor speed. With a frequency sweep from 0-1 Hz Figure 2.7 shows that the desired amplitude can be maintained only for lower frequencies before it declines. It is seen that at 0.3 Hz the system is no longer able to produce a 100% (106 cm) response. This model can be used to determine the maximum measurement range with a certain tractor speed and cycle rate or the maximum tractor speed for a certain measurement range and cycle rate.

For example, the command signal for the simulation that produced Figure 2.8 was set to produce an oscillation from 20-40 cm which is the region the hardpan is typically found [11]. Figure 2.8 shows the frequency being swept from 0-3 Hz. It

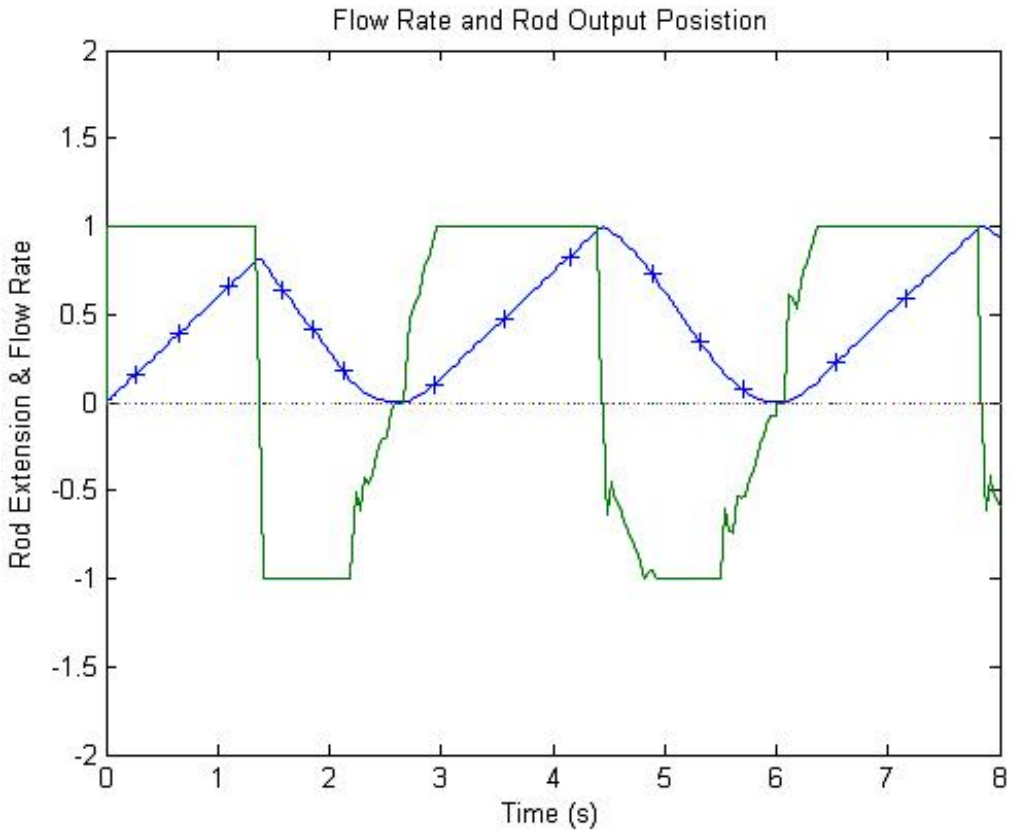

Figure 2.6: Normalized output position and normalized flow rate plotted together. The blue (+) is the response while the black line is the flow rate.

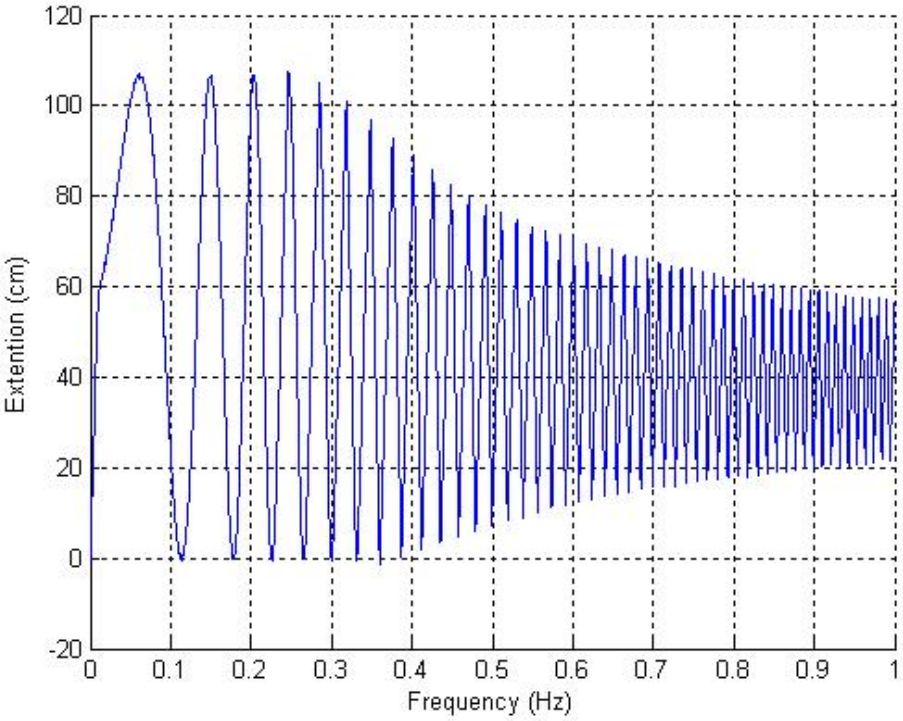

Figure 2.7: Position as a result of the chirp signal. The input starts a 0.0 Hz and increases to 1.0 Hz. And full stroke.

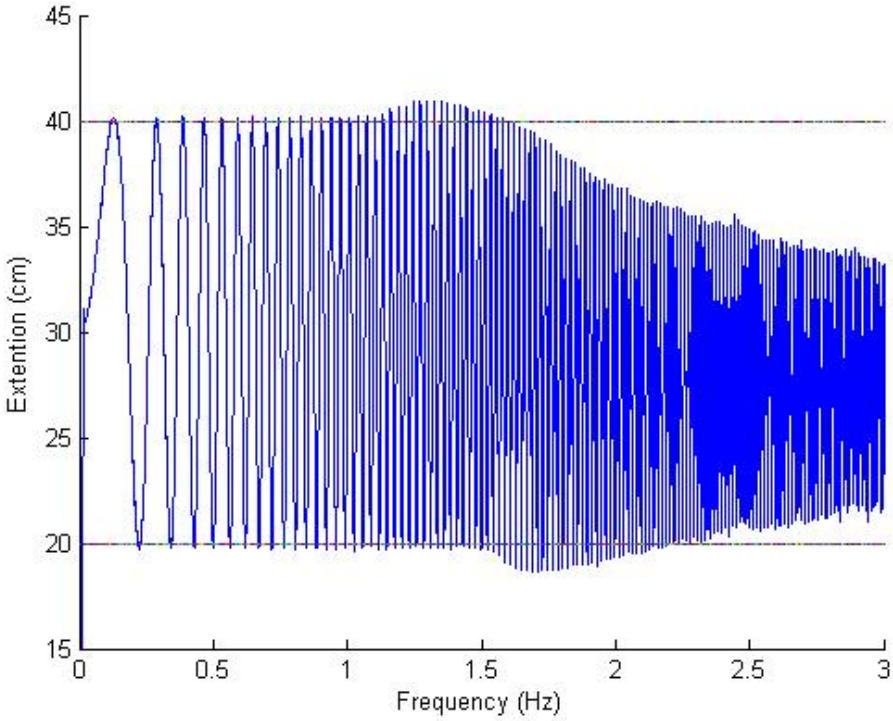

Figure 2.8: Chirp signal from 0-3 Hz. And 20 cm stroke.

can be seen that the system has a favorable response until about 1.5 Hz where the system seems to go unstable with unpredictable results. The frequency is directly proportional to the tractor speed and indirectly proportional to the cycle rate. A frequency of 1.5 Hz will be seen at two combinations of the speed rate ratio. A three dimensional surface plot was created to show the limits of the system.

2.4.5 The plot

Using information from the simulation and Excel's trend line function a piecewise function (see Equation 2.3) was created. With this function we were able to calculate the maximum range given at a certain rate and speed. A matrix similar to Figure 2.9 was created with this piecewise function and used to create the surface plots in Figure 2.10.

$$y = \begin{cases} 104.4 & x < 0.24 \\ 2301.3 * x^3 - 2674.4 * x^2 + 853.95 * x + 20.56 & 0.25 < x < 0.44 \\ 32.603 * x^{-1.008} & 0.45 < x \end{cases} \tag{2.3}$$

With similar surface plots we can determine the tractor speed and cycle rate allowable for a desired measurement range. More importantly, the piecewise function used to create the surface plots can be programmed into the software to control the command signal and to provide information to the operator. For example, a scientist or farmer could "tell" the control program that the system should cycle every 3 m at a depth of 25-50 cm. As the operator drives the tractor at a comfortable speed the program will control the amplitude and frequency of the tine to achieve this goal. The software program will also warn the driver when the tractor speed exceeds the limits and makes that goal unachievable.

		Tractor speed (m/s)										
		0	3	6	9	12	15	18	21	24	27	30
m/cyc		NaN	104	104	104	104	104	104	104	104	104	104
1		0	93	104	104	104	104	104	104	104	104	104
2		0	49	93	104	104	104	104	104	104	104	104
3		0	33	66	93	103	104	104	104	104	104	104
4		0	24	49	74	93	102	104	104	104	104	104
5		0	0	39	59	79	93	101	104	104	104	104
6		0	0	33	49	66	82	93	100	103	104	104
7		0	0	28	42	56	70	84	93	99	102	104
8		0	0	24	37	49	61	74	85	93	99	102
9		0	0	22	33	44	55	66	76	86	93	98
10		0	0	0	29	39	49	59	69	79	87	93

Figure 2.9: Measurement range given tractor speed and cycle rate.

2.5 Conclusions

The OSSS system was modeled using Mathworks MATLAB and SIMULINK. The dimensions of the hydraulic cylinder and the values of the amplifier parameters were used to simulate the response of the OSSS system. Through a simulation study, we have come to the conclusion that two issues must be considered in the control system:

- limited flow capacity from the tractor - limits the slew rate and bandwidth of the OSSS.
- valve deadband - affects positioning accuracy at low signal levels.

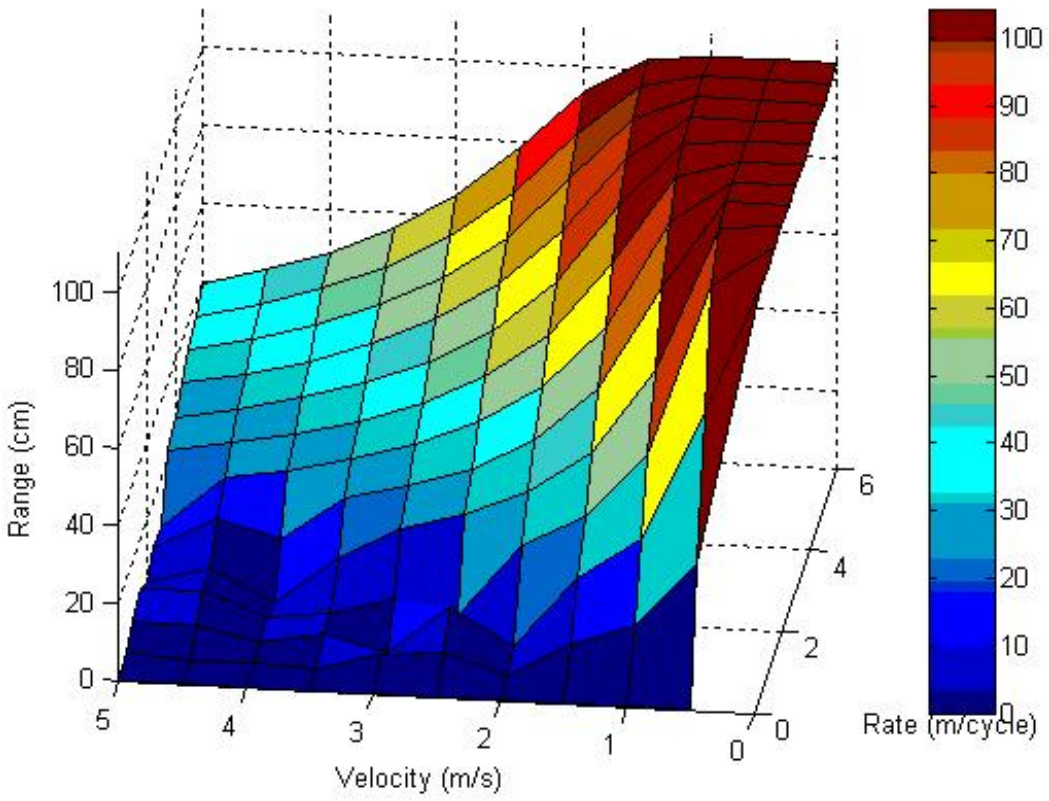

Figure 2.10: Three dimensional plot of system limits

Chapter 3

Control System Design and Implementation

3.1 Introduction

In order for the OSSS to work it needs a control system which will drive the OSSS and make it perform its oscillation task. This closed-loop control system consists of a computer program, an amplifier, an A/D converter, and a displacement sensor.

One of the goals of the design is to minimize human interaction, thus freeing the operator to drive the tractor. Therefore, a control program was designed to handle the input/output signal processing. The control program controls shank/tine oscillation and data collection according to predetermined inputs from the operator and the tractor speed. The controller is designed and constructed to run on a laptop computer using LabVIEW version 7.1. The simple block diagram of the control scheme is shown in Figure 3.1.

3.2 The Block Diagram Flow

The "command" signal is generated in the control software and sent to the Proportional, Integral, and Derivative (PID) Module via an electronic data acquisition card and the printed circuit field connector board. A signal from the PID module controls the solenoid valve (a part of the "plant" block). The system receives shank

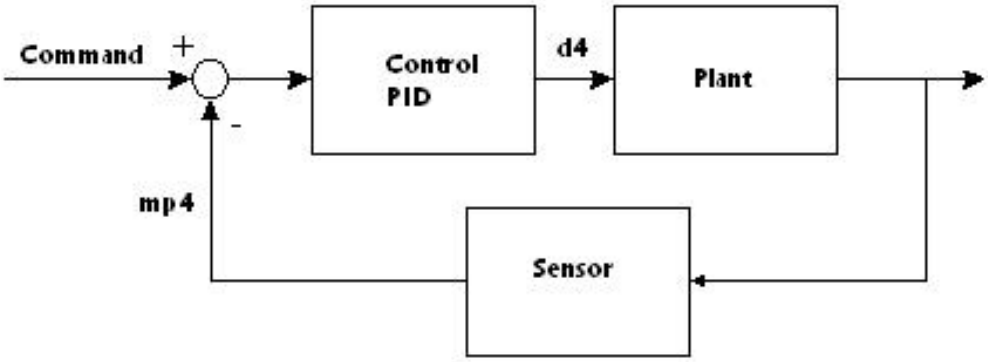

Figure 3.1: Block diagram of the control system

position feedback from the draw wire sensor. The PID controller compares the measured shank position "mp4" against the "command," and automatically produces the control signal "d4". The PID module produces a control signal based upon three components: instantaneous error, rate of change of feedback, and error accumulated over time. The relative weight to each component is to be determined in future work, and depends upon the dynamic capabilities and performance requirements of the OSSS system. The Flow chart for the control system is shown in Figure 3.2.

3.3 Command Signal Output

3.3.1 DGPS to Calculate Oscillation Frequency

When the system is in run mode, DGPS (Differential Global Positioning System) information is read through the serial port on the computer. This information is used

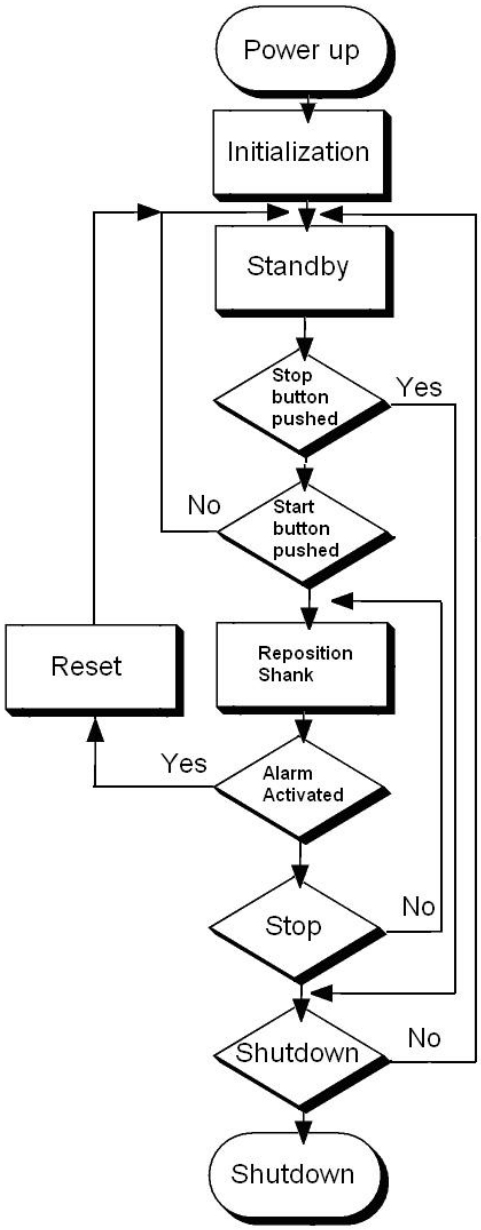

Figure 3.2: Flow Chart

to calculate the shank oscillation frequency, using the tractor speed. The DGPS transmits signals according to the National Marine Electronics Association standard (NMEA 0183) in the form of hexadecimal strings via serial RS232 cable. A portion of the control system is designed to read the NMEA information from the serial port and rebuild the NMEA sentences received from the DGPS receiver. The "NMEA read" algorithm reads one hexadecimal byte from the serial input and compares the values to standard NMEA tokens. Each NMEA string begins with a "$GP" (24 hex) and every time this symbol is found, a new line is created. The next bytes (separated by commas) are read and stored on this line until another "$GP" is found. The next set of information indicates which NMEA string is being read. Although there are several NMEA strings to choose from, the RMC (recommended minimum) string has latitude, longitude, and speed information and is the only one used by the software program. The latitude and longitude information will be stored with the soil strength data and the speed is used for the oscillation frequency calculation. The DGPS algorithm looks for the RMC string alone, and the rest are ignored. The RMC information is parsed out of the rest of the NMEA information. The speed is sent to the frequency calculation algorithm and the coordinate information is stored to a file with the data.

3.3.2 Command Voltage

This command signal is an incremented sinusoidal voltage calculated from the horizontal distance traveled by the tractor and the cycle rate.

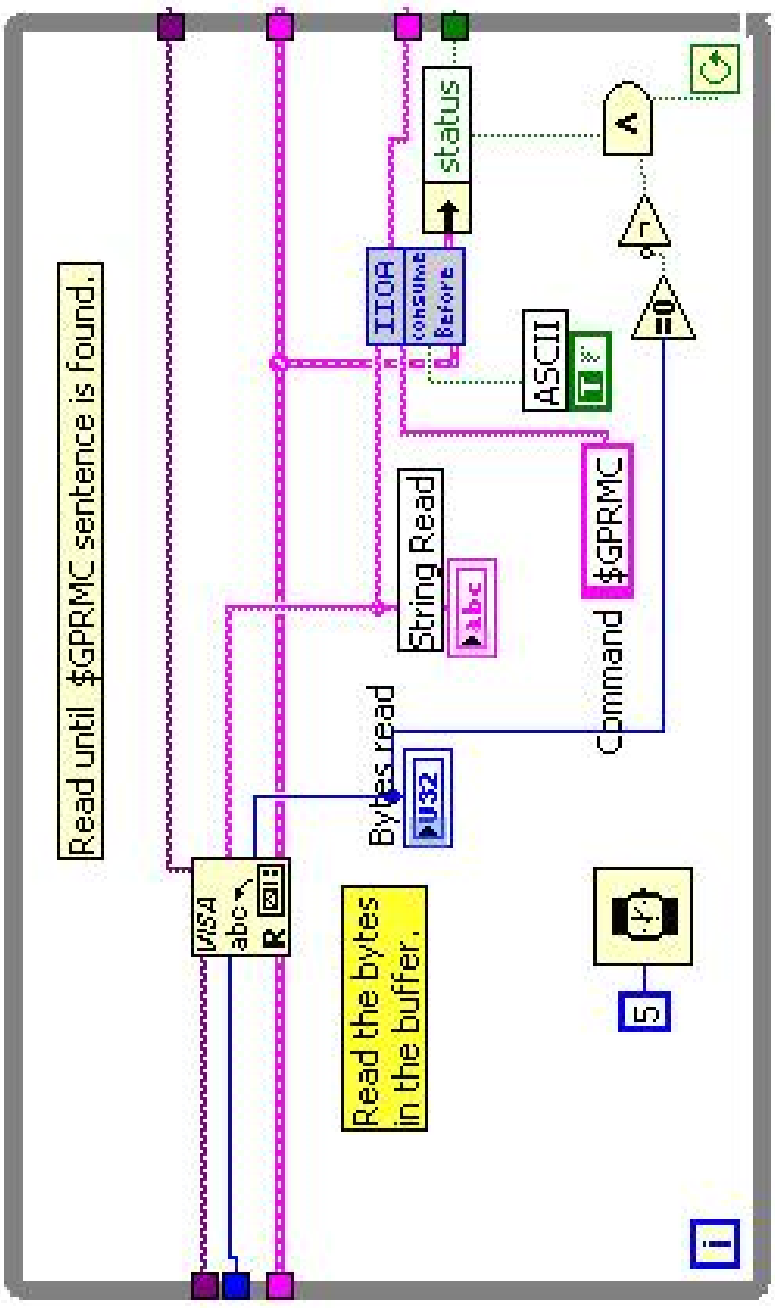

Figure 3.3: Algorithm to collect RMC sentence

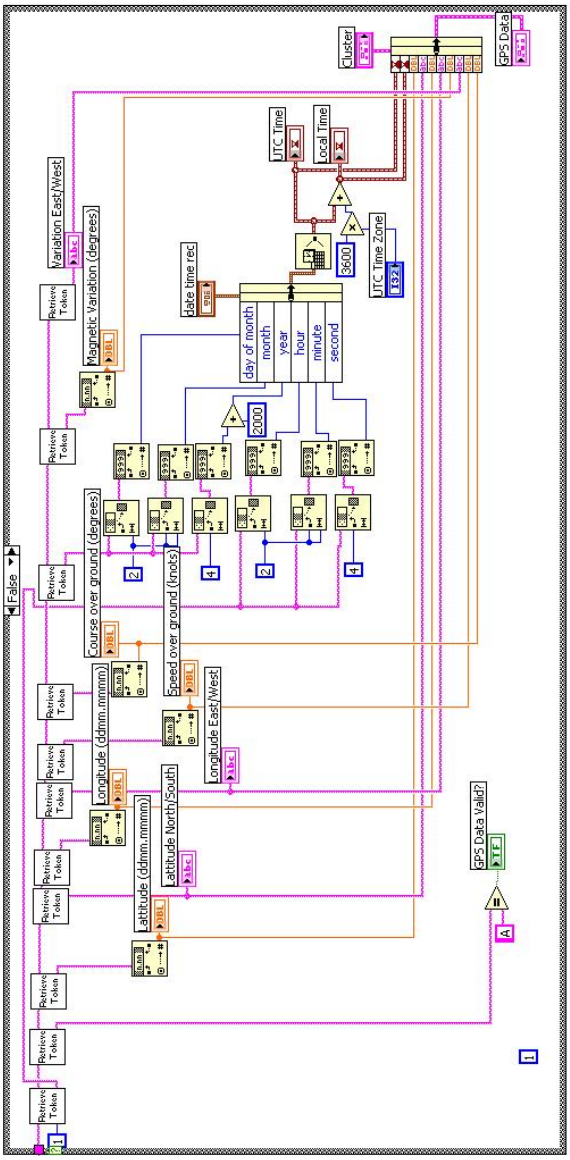

Figure 3.4: Algorithm to parse RMC in LabVIEW

Figure 2.1 shows how OSSS will oscillate. Using the speed information from the DGPS, the command signal voltage is recalculated for the shank movement. The algorithm that collects the speed information runs at about 0.5 Hz so there is a 2 second delay between each speed adjustment. The speed is divided by the time (recorded by the computer) since the last speed adjustment to get the distance traveled. The equation used to calculate the voltage output is:

$$VS = R * \sin(\pi \times (DT - CR \times \lfloor DT/CR \rfloor)) + Z \tag{3.1}$$

Here VS is the command voltage, DT is the distance traveled by the tractor, and CR is the cycle rate which is the distance traveled by the tractor per shank oscillation set by the operator. R is the measurement range set by the operator, and Z is the depth of measurement set by the operator. Once the command signal is calculated it is routed to the amplifier through the data acquisition card.

3.3.3 System Startup and Configuration

Under normal circumstances the operator will control only power up, start, stop and shutdown while the control program handles all major tasks associated with each command. For the operator these are one button commands requiring minimal concentration. The software program controls toggling of individual digital channels that control the PID module, the analog signal that positions the shank and everything

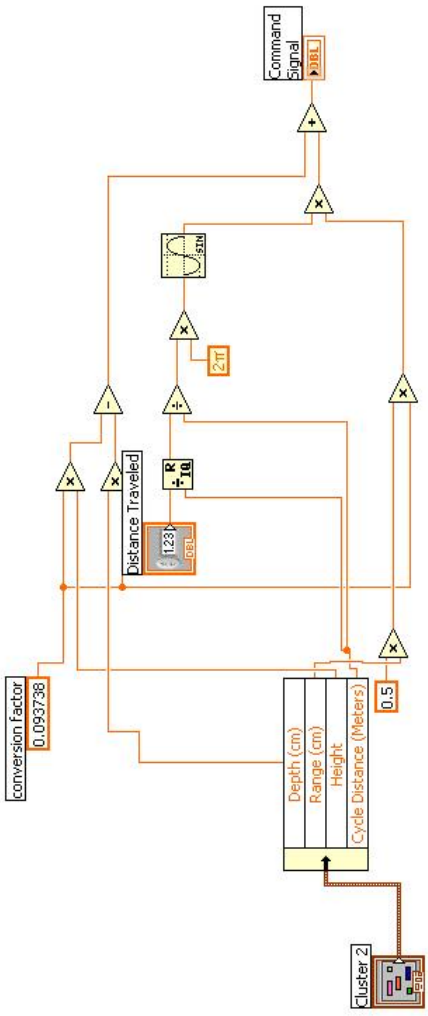

Figure 3.5: Command signal calculator in LabVIEW

else including system monitoring, oscillation frequency, and data collection. The user interface for the OSSS system is shown in Figure 3.6.

This screen shot shows what the operator sees while using the OSSS system. On the right side of the user interface is the configuration section, where the measurement configurations are set by the operator. In the configuration section, operating test parameters can be employed to determine if the system is functioning properly. The section to the left is designed to be similar to the front panel of the Vickers amplifier. Most status LED's on the amplifier can be read on the user interface. Most of the information from the monitoring points on the front panel is displayed for the operator. The PID, ramps, and deadband adjustment points can not be controlled from the control program and are not available on the user interface. The command signal gauge in the middle of the simulated amplifier is not available on the actual amplifier. This two marker gauge shows the command signal output with one marker and the displacement sensor input with the other. The OSSS system is enabled from this section of the user interface.

At the start of the system, the operator starts the OSSS with the "Power Up" button on the user interface. After the operator powers up the system he/she waits for the "Initialization Progress" to complete. In the mean time, the system runs the initiation sequence and checks necessary parameters for the system. The PID module is turned on, followed by a delay before the drive and the PID are enabled. When the system becomes stable the integrator is enabled[1]. Immediately after the

[1]This delay before the integrator is enabled prevents pressure spikes in the hydraulic system.

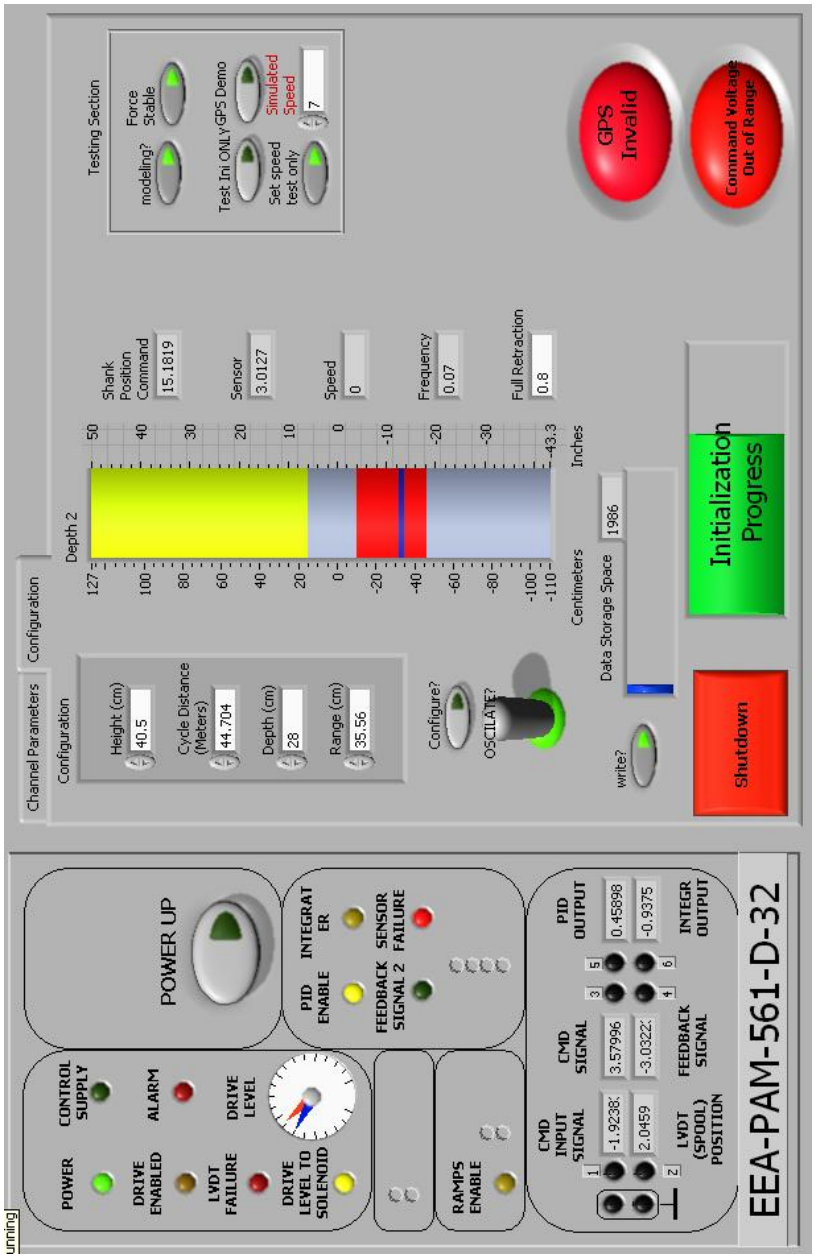

Figure 3.6: OSSS's user interface

initialization progress completion, the OSSS system goes into a ready/standby mode. In this "ready" mode the analog and digital channels as well as the DGPS signals are monitored. This information is available to the operator on the front panel of the control program.

While in the "ready" mode the measurement configuration is to be set. The measurement configuration section located close to the middle of the user interface was designed to be as simple as possible. The values set in the measurement configuration determine the depth, range and frequency of the shank oscillation. The parameters to be set are:

- Height-the distance from the OSSS sensor to the soil surface while the OSSS cylinder is fully retracted. Units are in *cm*.
- Cycle distance-the distance traveled by the tractor for OSSS oscillation
- Depth-the average distance of the hardpan beneath the soil surface
- Range-the amplitude of the OSSS oscillation

The vertical fill slide located to the right of the configuration section is a display of the measurement settings. This visual aid allows the operator to see how the measurement parameters will affect the shanks motion. In the configuration mode the operator can see if the shank will travel out of the soil or if the measurement settings make sense. When the OSSS is oscillating the fill slide will show the OSSS shank position.

3.3.4 Operation Mode

After the system has been powered-up and the measurement configuration have been set, the operator is ready to start collecting data. The data collection sequence is started when the "Oscillation" and "Write" switches are turned on. The "Oscillation" toggle switch in the up position allows the command voltage to be updated and sent to the amplifier. At the end of a pass the operator will stop the system using the "Oscillate" switch. When the "Oscillate" switch is down the system will stop. In the stop sequence, the shank is raised out of the soil in preparation for any turning of the tractor and the data storage is halted. The system will return to the ready mode and await the next command. The "Shutdown" button is employed when the OSSS is to be turned off. The shutdown button also works as the emergency stop if it is activated before the "Oscillate" switch is toggled down. When the shutdown command is given, the program will send a signal to raise the shank and the PID module will be turned off. After the shutdown/emergency stop button is employed, the system will have to go through the power up sequence before the start/data collection button can be read.

The operation mode consists of two sequences: data collection and command signal output. In the data collection sequence information from the digital inputs are monitored for alerts and warnings from the PID module. Analog data is collected from the circuit board, which includes PID module information and sensor information. The DGPS data is collected in this sequence as well. If the system is on standby mode, this information is only displayed on the front panel. When the start command is

activated, the information from the data collection sequence is used to calculate the command signal in the command signal output sequence. When the tractor stops the shank will stop and hold its position until either the tractor moves again or the stop sequence is initiated.

3.4 Deadband Compensation

Once the OSSS system was constructed and operational the issue of the deadband was addressed. Figure 3.7 shows the response of the system with factory set dead zone. It can be seen in Figure 3.7 that there is a delay in the response before the shank motion changes direction. This delay is the result of an excessive dead zone. On the front panel of the amplifier there are two potentiometers used to adjust the deadband. Figure 3.8 shows the response of the system after the dead zone was reduced. With the control system and the frame built the system can be tested.

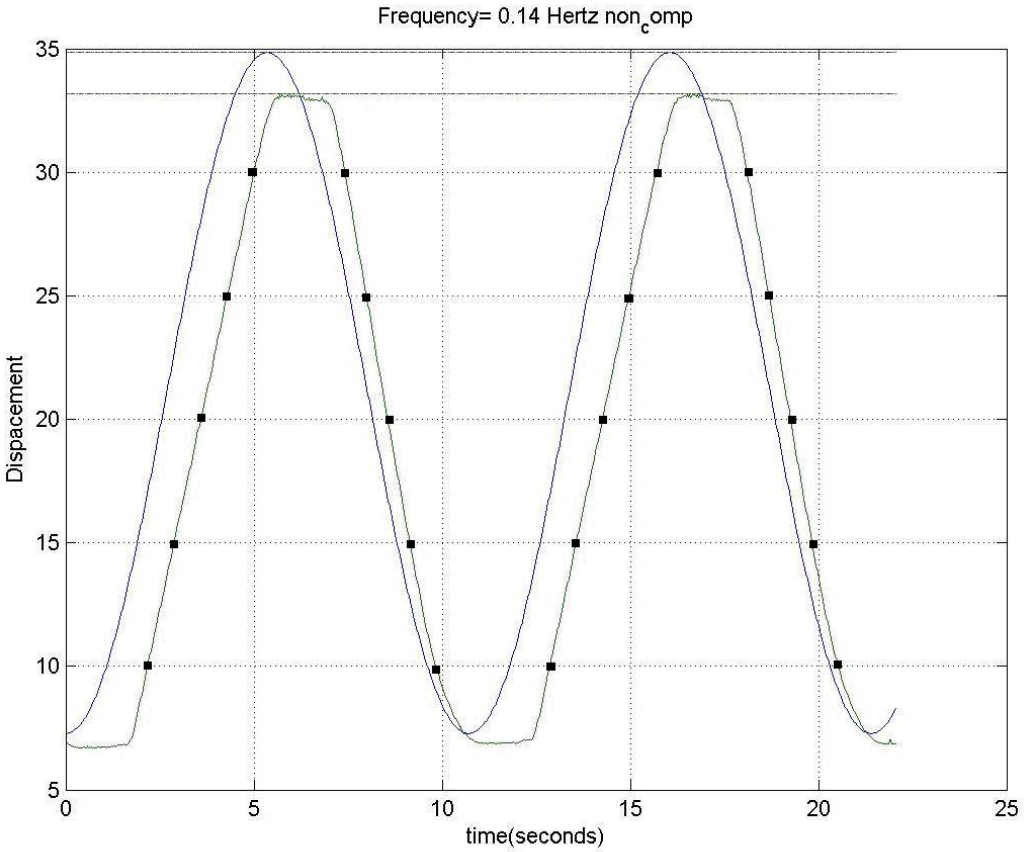

Figure 3.7: System with factory set deadband compensation. The solid line shows the input to the system. The dotted line shows the output movement of the shank with no deadband compensation in the amplifier.

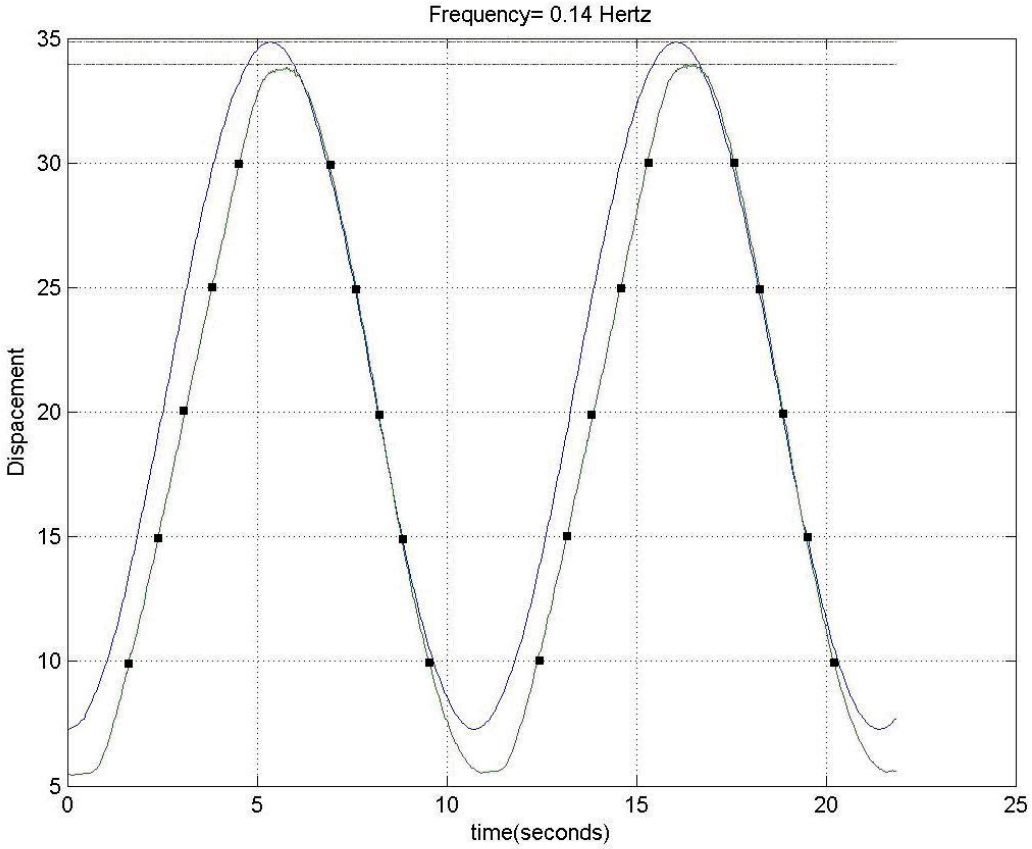

Figure 3.8: System with deadband compensation adjustment in place. The solid line shows the input to the system. The dotted line shows the output movement of the shank with deadband compensation in the amplifier.

Chapter 4

Experimental Evaluation

The final step in the project is the system performance evaluation. To use the OSSS system safely and efficiently, the operator must be aware that the system has limits, as stated in chapter 2. To operate in a range beyond these limits would be dangerous. And to operate the system too far below these limits would waste time. The purpose of this chapter is to explore the operational limits of the physical system. This was done through the evaluation of the frequency response for the project results.

4.1 Experimental Approach

The OSSS system was first tested in a controlled environment (see Figure 4.1) with a stationary tractor. The OSSS shank was not attached to the OSSS frame, allowing the hydraulic cylinder to travel freely. In order to test the system response, a set of frequencies ranging from .01 Hz to .5 Hz was used. To realize these frequencies the simulated speed was incrementally increased over time. The shank position was recorded with the command signal output, the oscillation frequency, and the PID controller output in an Excel spreadsheet. This information was used to evaluate the system.

Figure 4.1: OSSS Mechanics Attached to Tractor

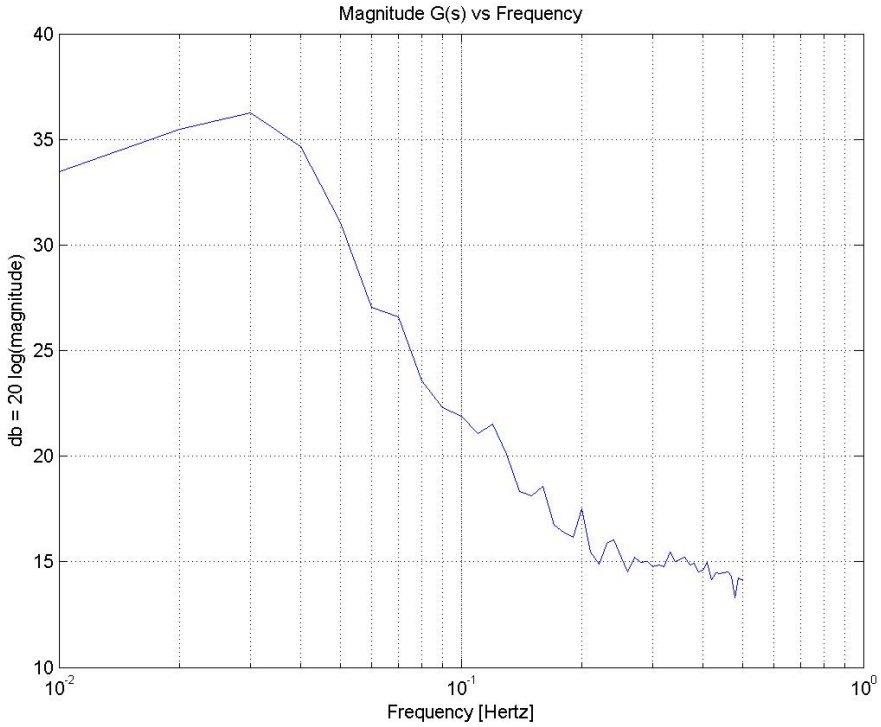

Figure 4.2: $G(s)$ (Open Loop Magnitude Response)

4.1.1 Step Response Tests

A step response is a typical experiment for this type of system. A step response experiment was attempted but the hydraulic pressure spike was too much for the hydraulic system to handle. The O-rings on the hydraulic connection could not withstand the pressure spike and ruptured during the test process. Therefore, no step response information is presented.

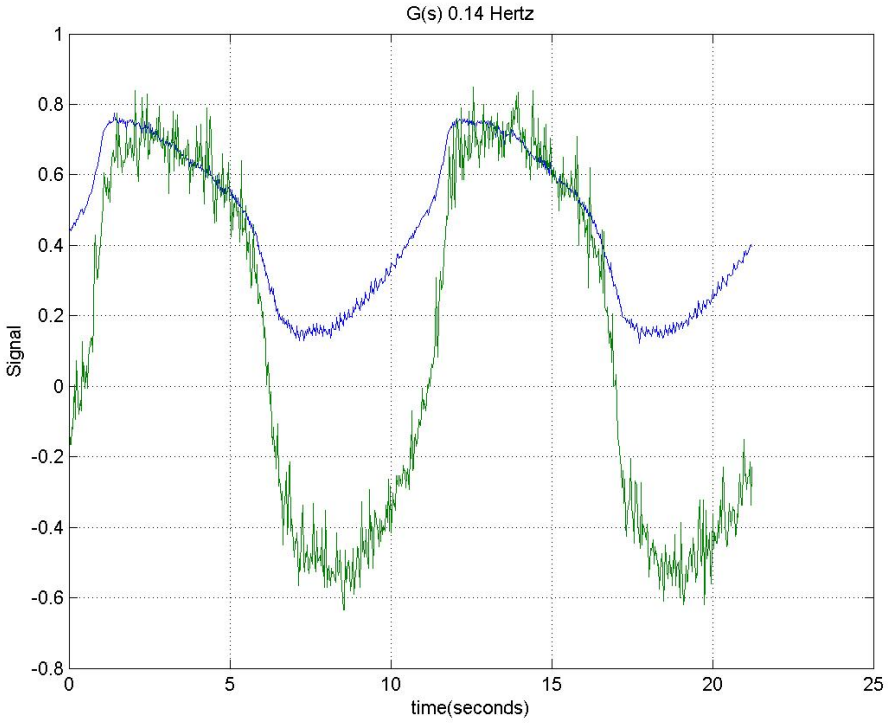

Figure 4.3: $G(s)$ Open Loop response.

4.1.2 Plant Frequency Response

In this work, the "plant" is considered to be that part of the feedback loop lying between the PID controller output and sensor output. The output of the PID controller is the input to the plant, which is denoted $G(s)$. A plot of the experimentally measured frequency response $G(\omega)$ can be seen in Figure 4.2. An approximate transfer function model fitted to the model would be first order, with a bandwidth approximately 0.03 Hz.

$$G(s) = \frac{Y(s)}{U(s)} \tag{4.1}$$

4.1.3 PID Controller Response

A plot of the PID output signal and the sensor input can be seen in Figure 4.3. The noisy line in the sensor and the other line is the PID output. Much of the noise in the sensor signal is due to the jerkiness of the rapid opening and closing of the valve. At higher frequencies the cylinder is trying to keep up with the command signal, therefore, the fluid through the cylinder is allowed to flow at rated flow rate and the vibrations are greatly reduced.

4.1.4 Closed Loop Response

The closed loop transfer function is given by (4.2)

$$H(s) = \frac{Y(s)}{R(s)} = \frac{C(s)G(s)}{1 + C(s)G(s)}$$

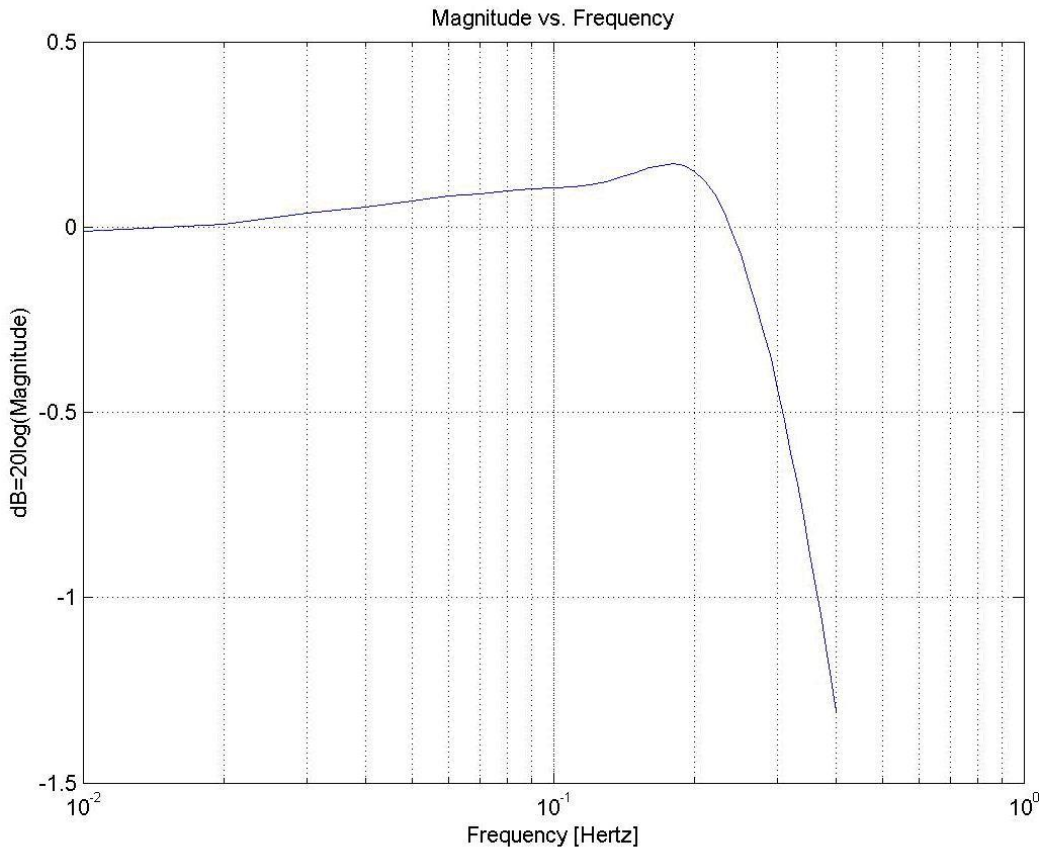

Figure 4.4: Closed loop frequency response (Simulated)

The simulated closed loop frequency response is shown in Figure 4.4. The experimentally measured response is shown in Figure 4.5, and it matches the simulated response quite well. The closed loop system bandwidth is approximately 10 times higher than the open loop bandwidth. For reference purposes, the measured phase response of the system is shown in Figure 4.5. The phase response can be used to predict the delay between the commanded position and actual position of the OSSS.

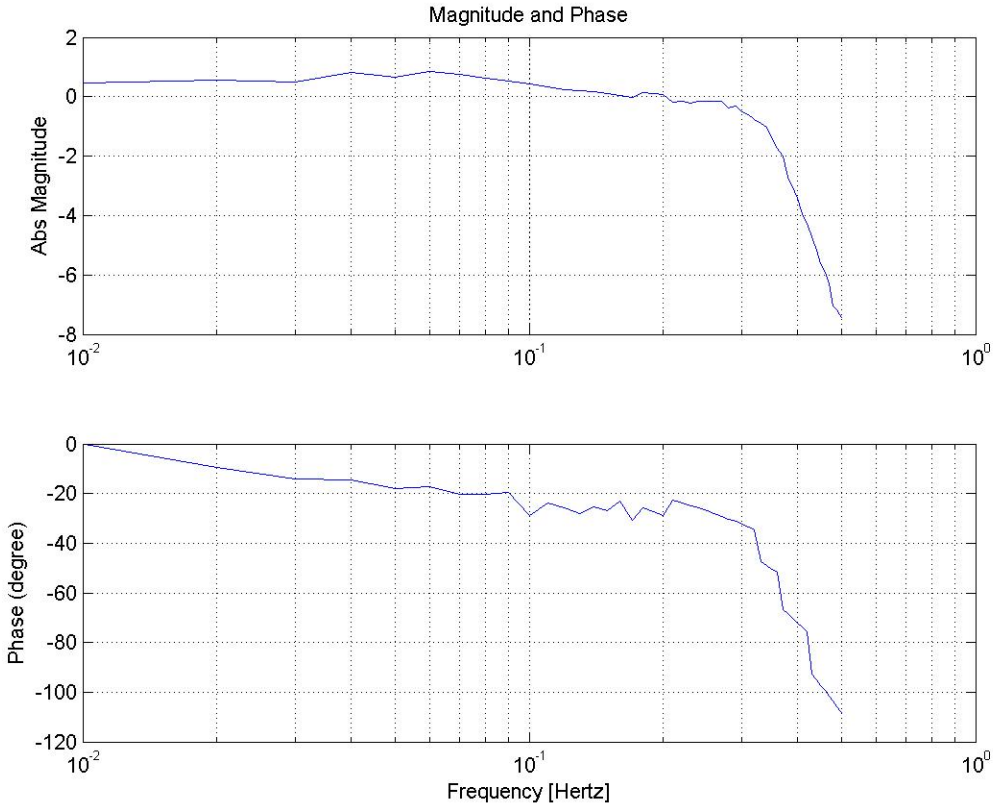

Figure 4.5: Closed loop frequency response (Measured)

4.1.5 OSSS In The Field

An experiment was conducted to test the OSSS in a field environment. The oscillating frequency was set at 0.272727 Hz (period of 3.667 seconds). The OSSS was pulled for about about 30s under closed loop control with the tine oscillating beneath the soil surface. Figure 4.6 shows some the information from that was acquired from that field test. The draw wire sensor output has a voltage bias that can be subtracted out. The phase difference between the reference and output is consistent with the experimentally measured frequency response (see Fig. 4.5).

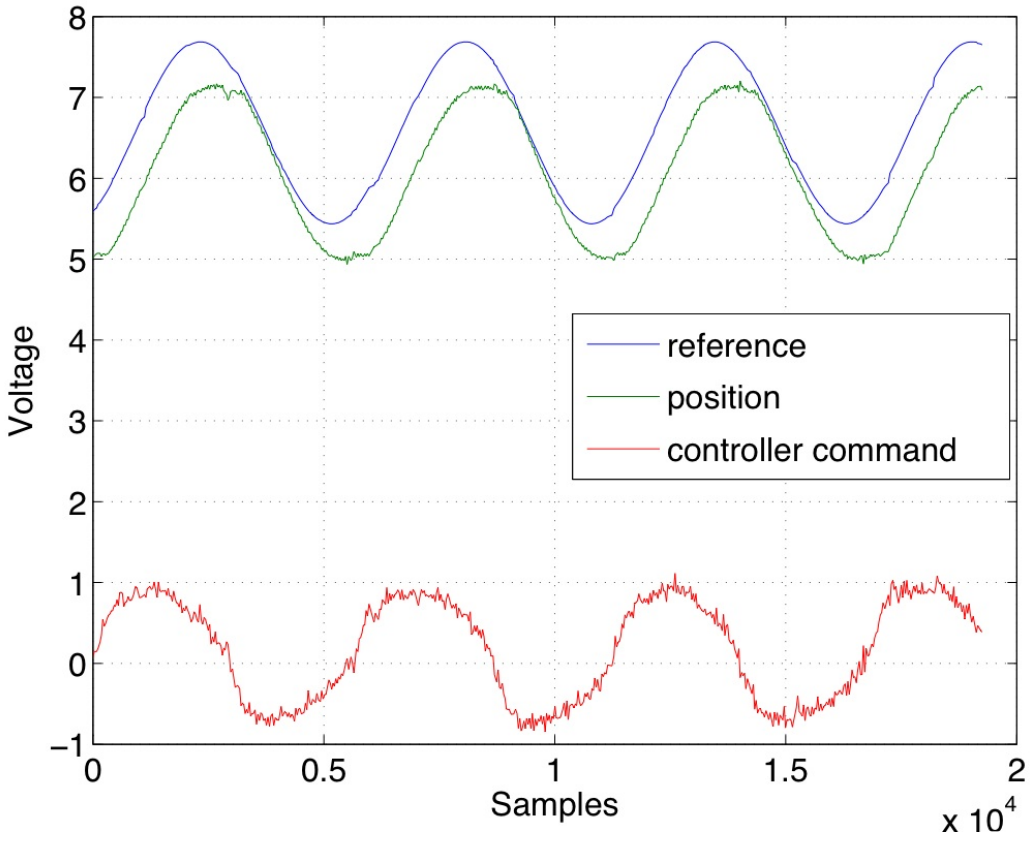

Figure 4.6: Closed Loop Response (collected in the field)

Chapter 5

Conclusions and Future Work

5.1 Summary

The focus of this thesis was the design implementation and evaluation of the automatic depth control system for the on-the-go method of sensing soil strength (OSSS). The software was designed and implemented with LabVIEW 7.1 to drive a PID controller for a hydraulic cylinder. This system oscillates a shank in the soil at consistently spaced intervals regardless of tractor speed variations. The control system and the hardware have been designed for the OSSS.

5.2 Future Work

A controller has been designed and built to operate the OSSS. This controller will maintain the amplitude and frequency necessary to measure the soil strength profile. The control system is designed and the integration of the software and hardware are complete and verified. Future work could include determination of optimal PID controller tunings, and completion of the data collection algorithm.

Testing reveals that the closed loop bandwidth of the system is limited by the flow capacity of the hydraulic system. Higher bandwidth (the ability to oscillate more quickly) requires that the hydraulic cylinder move more quickly. A smaller diameter cylinder would yield faster response, at the expense of decreased force available to

lower or raise the OSSS. An alternative would be to increase the hydraulic pump capacity, but that may likely require significant modification to the tractor.

Appendices

Appendix A
The Printed Circuit Board

A.1 37 Pin Connector

A.2 9 Pin Connector

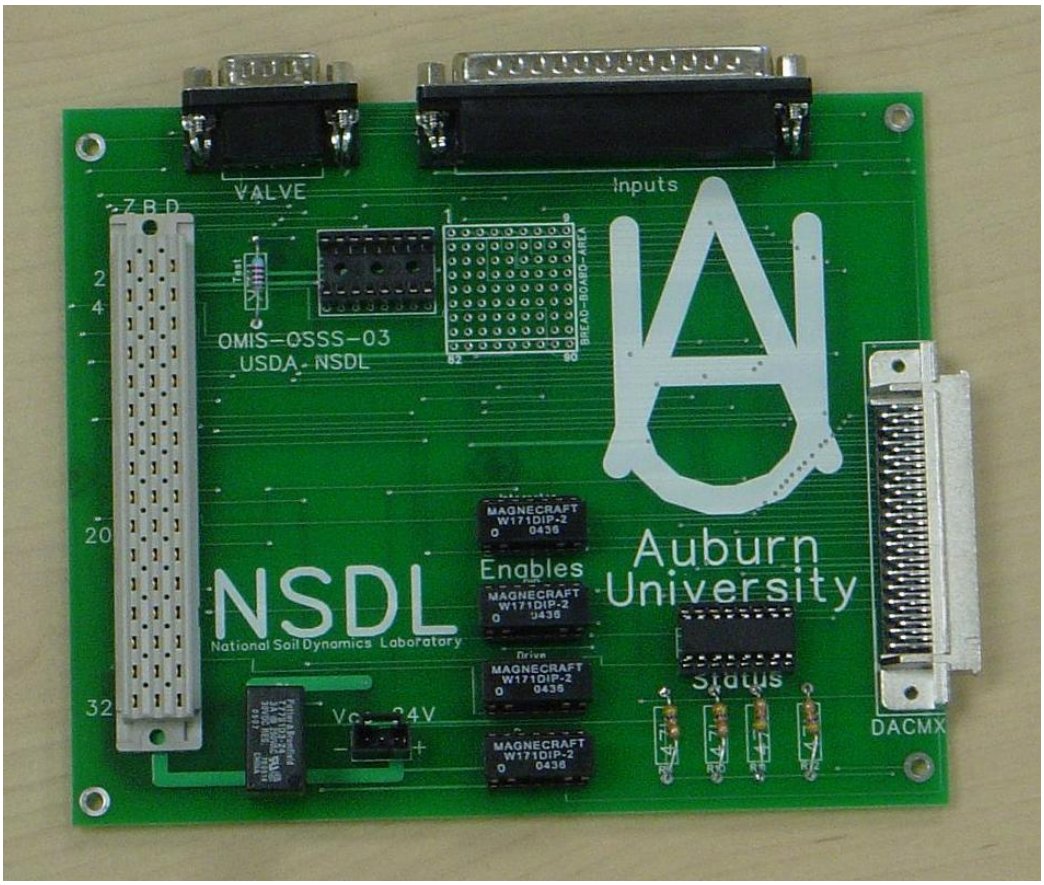

Figure A.1: Printed Circuit Board

Table A.1: 37 Pin Connector

BD PIN#	CONN PIN#	SIGNAL	TERMINAL
1	19	AIGND	DAQ.69
2	18	COMMAND SIGNAL	AMP.B6
3	17	ACH9	DAQ.66
4	16	ACH10	DAQ.31
5	15	ACH11	DAQ.63
6	14	ACH12	DAQ.61
7	13	ACH13	DAQ.26
8	12	ACH14	DAQ.58
9	11	ACH15	DAQ.23
10	10	SOLENOID	AMP.Z28
11	9	SOLENOID	AMP.Z26
12	8	-10 REF	AMP.B2
13	7	+10 REF	AMP.Z2
14	6	5B MODULE CHB	DAQ.33
15	5	5B MODULE CHA	dup
16	4	AIGND	DAQ.68
17	3	DGND	DAQ.13
18	2	+5_0	DAQ.14
19	1	AOGRND	DAQ.54
20	37	AIGND	DAQ.69
21	36	+5_1	DAQ.8
22	35	AIGND	NONE
23	34	SNESOR	DAQ.57, AMP.D2
24	33	GROUND	GROUND
25	32	24v	Vcc
26	31	AISENCE	DAQ.62
27	30	CURRENT COMMAND	AMP.Z6
29	28	SENSOR mA	AMP.D6
31	26	INVERTED COMMAND INPUT	AMP.Z10
28,30,32,36	29,27,25,21	GROUND	UNCONNECTED
33	24	DV1	AMP.B8
34	23	DV2	AMP.Z8
35	22	DV3	AMP.B10
37	19	UNCONNECTED	UNCONNECTED

Table A.2: 9 Pin Connector

PIN#	SIGNAL	TERMINAL
1	SOLENOID	AMP.Z28
2	SOLENOID	AMP.Z26
3	LVDT PIN1	AMP.B14
4	LVDT PIN2	AMP.Z22
5	LVDT PIN3	AMP.B16
6	GROUND	GROUND
7	GROUND	GROUND
8	LVDT PIN2	TEST.2 [1]
9	LVDT PIN3	AMP.Z22

Appendix B
The Frame

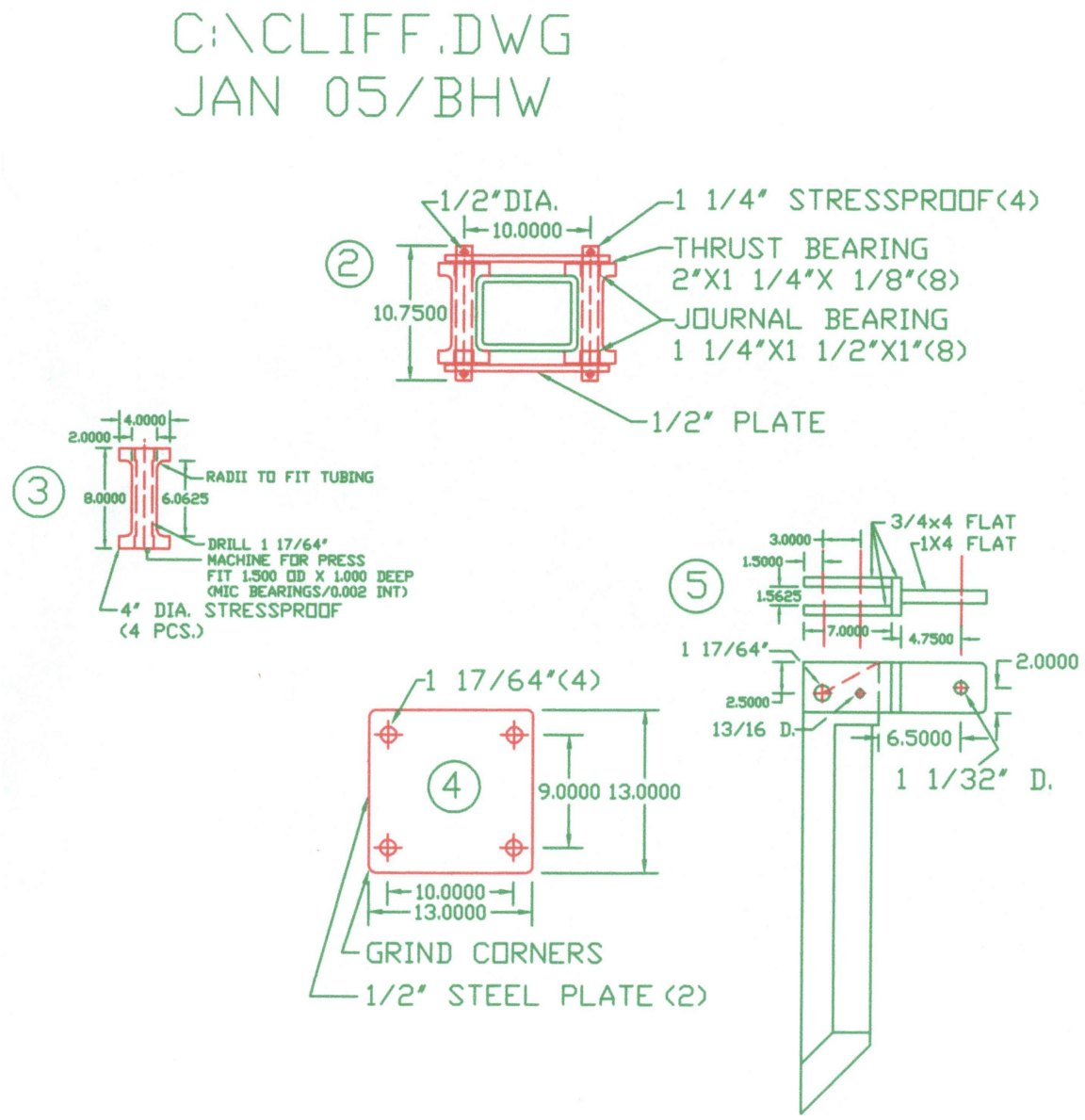

Figure B.1: Frame1

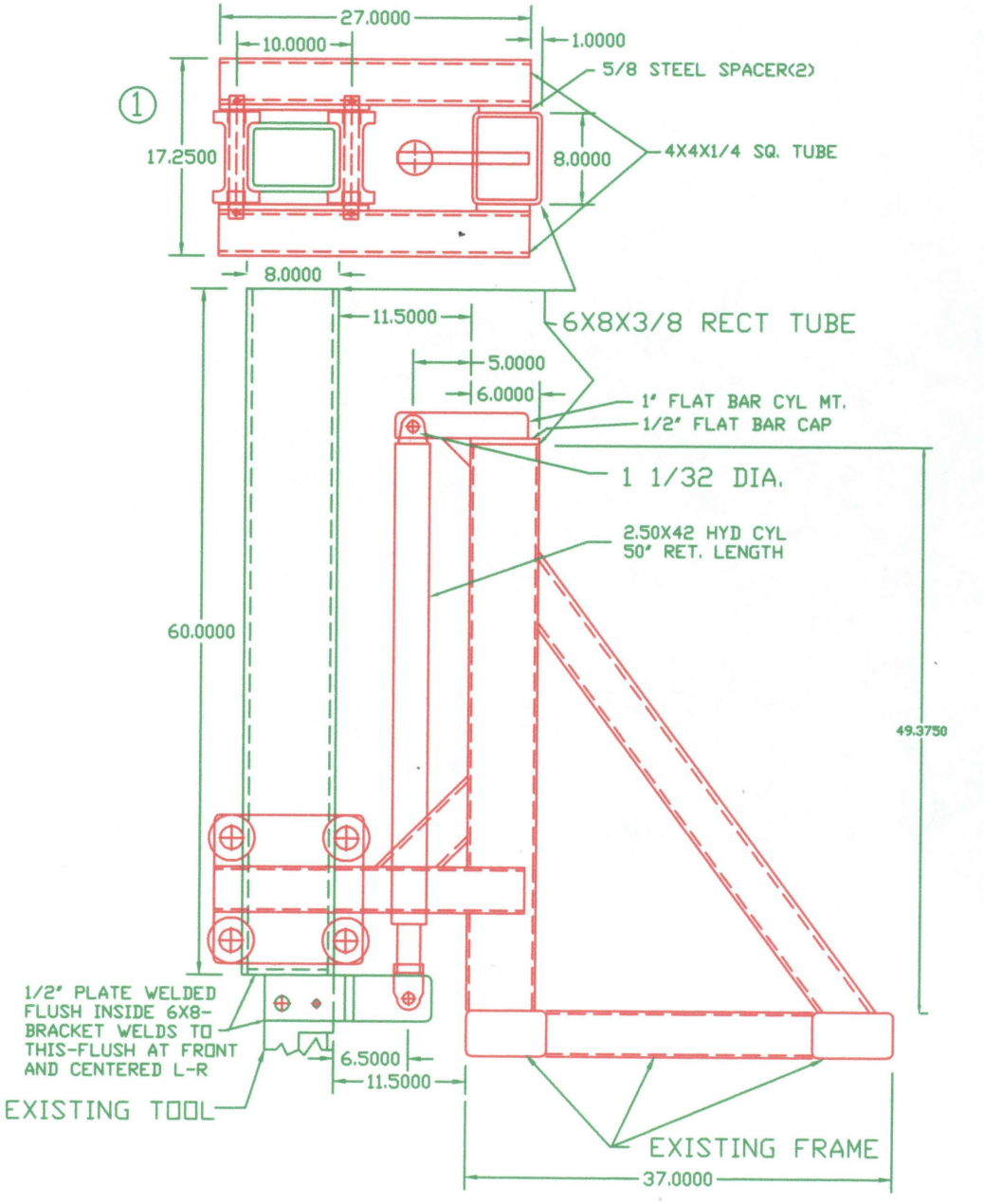

Figure B.2: Frame2

Bibliography

[1] "ASAE standard," S313.3 Cone Penetrometer. St. Joseph, MI, 2004.

[2] R. L. Raper, B. H. Washington, and J. D. Jarrell, "A tractor-mounted multiple-probe soil cone penetrometer," Applied Engineering in Agriculture, vol. 15, no. 4, pp. 287–290, April 1999.

[3] T. Alihamsyah and J. E. G. Humphries, C. G. Bowers, "A technique for horizontal measurement of soil mechanical impedance," American Society of Agricultural Engineers, vol. 33, no. 1, pp. 73–77, January 1990.

[4] Acoustic Compaction Layer Detection, no. 021089, Chicago, Illinois, USA, July 2002.

[5] V. I. Adamchuk, M. T. Morgan, and H. Sumali, "Applications of a strain gauge array to estimate soil mechanical impedance on-the-go," Transactions of the ASAE, vol. 44, no. 6, pp. 1377–1383, 2001.

[6] G. Manor and R. L. Clark, "Development of an instrumented subsoiler to map soil hard-pans and real-time control of subsoiler depth," in ASAE Annual International Meeting. Sacramento, CA: ASAE, July 2001.

[7] E. Chukwu and C. G. Bowers, "Instantaneous multiple depth soil mechanical impedance sensing from a moving vehicle," Transactions of the ASAE, vol. 48, no. 3, pp. 885–894, 2005.

[8] On-the-go Soil Strength Profile Sensor Using a Load Cell Array, no. 031071. Las Vegas, NV: ASAE, July 2003.

[9] P. Andrade, S. Upadhyaya, B. Jenkins, and A. G. S. Filho, "Evaluation of the uc davis compaction profile sensor," in ASAE Annual International Meeting / CIGR XVth World Congress. Chicago, IL: ASAE, July 2002.

[10] A. Abou-Zeid, R. L. Kuchwaha, and D. S. D. Stilling, "Distributed soil displacement associated with surface loading," in ASAE Annual International Meeting. Las Vegas, NV: ASAE, July 2003.

[11] R. L. Raper, E. B. Schwab, and S. M. Dabney, "Measurement and variation of site-specific hardpans," American Society of Agricultural Engineers, Tech. Rep. 01-1008, July 2001.

[12] L. G. Wells, T. S. Stombaugh, and S. A. Shearer, "Crop yield repsonce to precision deep tillage," in 2003 ASAE Annual International Meeting, no. 031083. Las Vegas, Nevada, USA: ASAE, July 2003.

[13] R. L. Raper, D. W. Reeves, J. Shaw, E. van Santen, and P. Mask, "Effect of site-specific tillage on draft requirements and cotton yield," in Beltwide Cotton Conferences, January 2003, pp. 2025–2028.

[14] H. E. Hall and R. L. Raper, "Development and concept evaluation of an on-the-go soil strength measurement system," Transactions of the ASAE, vol. 48, no. 2, pp. 469–477, February 2005.

[15] R. L. Raper, "Soil compaction management," Encyclopedia of Agricultural, Food, and Biological Engineering, pp. 902–905, August 2003.

[16] V. I. Adanchuk, A. V. Skotnikov, J. D. Speichinger, and M. F. Kocher, "Development of an instrumented deep-tillage implement for sensing of soil mechanical resistance," Transactions of the ASAE, vol. 47, no. 6, pp. 1913–1919, 2004.

[17] J. V. Perumpral, "Cone penetrometer applications – a review," Transactions of the ASAE, vol. 30, no. 4, pp. 839–944, July 1987.

[18] J. R. Williford, O. B. Wooten, and F. E. Fulgham, "Tractor mounted field penetrometer," Transactions of the ASAE, vol. 15, pp. 226–227, 1972.

[19] R. R. Price and J. Theriot, "Development of a frame to automatically insert a hand-held penetrometer," in ASAE Annual International Meeting, no. 031077. Las Vegas, NV: ASAE, July 2003.

[20] H. E. Hall, "Development of an on-the-fly mechanical impedance sensor and evaluation in a coastal plains soil," Master's thesis, Auburn University, Auburn, Alabama, December 2001.

[21] P. Andrade, U. Rosa, S. Upadhyaya, B. Jenkins, J. Aguera, , and M. Josiah, "Soil profile force measurements using an instrumented tine," in ASAE Annual International Meeting. Sacramento, CA: ASAE, July 2001.

[22] J. L. Glancey, S. K. Upadhyaya, W. J. Chancellor, and J. W. Rumsey, "An instrumented chisel for the study of soil-tillage dynamics," Soil Till. Res., vol. 14, no. 1, pp. 1–24, 1989.

[23] R. L. Raper and H. E. Hall, "Soil strength measurement for site-specific agriculture," U.S. Patent No. 6647799, 2003.

[24] Vickers, Proportional Directional and Throttle Valves GB-C-2007C, Vickers Inc., April 1995.